UNIVERSITY
INSTITUTE
OF LISBON

Design and Evaluation of a Real-Time, Energy-Aware Wireless Pedestrian Counting Sensor Using Passive and Active Technologies

Tiago Filipe Alves Vieira

Master in Telecommunications and Computer Engineering

Supervisor:
PhD Rui Neto Marinheiro, Associate Professor,
Iscte – Instituto Universitário de Lisboa

Supervisor:
PhD Fernando Brito e Abreu, Associate Professor,
Iscte – Instituto Universitário de Lisboa

October, 2025

[This page has been intentionally left blank]

TECHNOLOGY
AND ARCHITECTURE

Department of Information Science and Technology

Design and Evaluation of a Real-Time, Energy-Aware Wireless Pedestrian Counting Sensor Using Passive and Active Technologies

Tiago Filipe Alves Vieira

Master in Telecommunications and Computer Engineering

Supervisor:
PhD Rui Neto Marinheiro, Associate Professor,
Iscte – Instituto Universitário de Lisboa

Supervisor:
PhD Fernando Brito e Abreu, Associate Professor,
Iscte – Instituto Universitário de Lisboa

October, 2025

[This page has been intentionally left blank]

Acknowledgment

First, I would like to express my sincere gratitude to my supervisor, Professor Rui Marinheiro, and my co-supervisor, Professor Fernando Brito e Abreu, for their invaluable guidance, continuous support, and insightful feedback throughout the development of this dissertation. Their dedication, availability, and encouragement were essential to completing this work successfully and to my personal and academic growth.

This work was carried out with the support of Instituto de Telecomunicações (IT-IUL), whose resources and research environment greatly contributed to the development of this dissertation.

Furthermore, I would like to acknowledge the support of project 2024.07624.IACDC/2024 funded by FCT – Fundação para a Ciência e a Tecnologia under PRR – Plano de Recuperação e Resiliência funding, investment RE-C05-i08 - Ciência Mais Digital, DOI: 10.54499/2024.07624.IACDC, and by national funds through FCT - Fundação para a Ciência e a Tecnologia, I.P., and, when eligible, co-funded by European Union funds under project/support UID/50008/2025 – Instituto de Telecomunicações.

I would also like to thank Tomás Santos, João Oliveira, and Miguel Martins, whose collaboration within a related research project made the experience both enriching and enjoyable.

A special thanks goes to my family, especially my parents and grandmother, for their constant patience, dedication, and support whenever it was needed.

Finally, I would like to express my gratitude to Rita Vieira, Diogo Mendes, and Bruno Pinhal for their continuous presence and friendship throughout this journey.

[This page has been intentionally left blank]

Resumo

A monitorização do fluxo de pedestres é essencial para o planeamento urbano, a gestão do transporte e as aplicações de cidades inteligentes. Em muitos contextos, deve ser realizada em ambientes com restrições espaciais, baixo volume de pedestres e infraestrutura limitada, incluindo ausência de energia e conetividade instável. Exemplos incluem observatórios de aves, áreas de conservação e locais históricos ao ar livre, onde soluções convencionais são impraticáveis.

Esta dissertação apresenta um sistema de contagem de pedestres economicamente e energeticamente eficiente, projetado para tais condições. O sistema integra dois pares de detectores infravermelhos ativos para registrar travessias e determinar a direção do movimento, enquanto sensores infravermelhos passivos ativam os detectores ativos e a unidade de processamento IoT. Esta estratégia reduz o consumo energético, operando apenas quando é detetado movimento. Para comunicação, o sistema seleciona dinamicamente entre Wi-Fi e LoRaWAN, garantindo flexibilidade de instalação.

A arquitetura combina software de código aberto e uso corrente, aumentando a reprodutibilidade e acessibilidade.

Foi realizado um estudo comparativo de vários detectores AIR, avaliando consumo energético, precisão, suscetibilidade à interferência e ângulo de feixe horizontal. Esta análise aborda a falta de avaliações sistemáticas de tecnologias de infravermelhos ativos para contagem de pedestres e fornece diretrizes para seleção de componentes em sistemas semelhantes.

Os resultados demonstram que o sistema proposto melhora a precisão e a eficiência energética, alcançando até 97% de precisão e um aumento de cinco vezes na autonomia operacional em relação às soluções convencionais com AIR, permitindo uma monitorização pedonal fiável, em tempo real e não intrusiva.

Palavras Chave: *Comparação de sensores infravermelhos*, *Contagem de pedestres*, *Redes de sensores de baixa potência*.

[This page has been intentionally left blank]

Abstract

Pedestrian flow monitoring is important for urban planning, transportation management, and smart city or tourism applications. Moreover, real-time monitoring may be essential in critical environments with low pedestrian volumes and limited infrastructure, including the absence of power supply and unreliable connectivity. Examples include birdwatching observatories, wildlife conservation areas, and open-air heritage sites, where conventional sensing solutions are impractical.

This dissertation presents a cost-effective and energy-efficient pedestrian real-time counting system designed for such conditions. The system integrates two pairs of active infrared detectors to register crossings and determine movement direction and counting, while passive infrared detectors activate both the AIR detectors and the Internet of Things processing unit. This strategy reduces energy consumption by enabling operation only when motion is detected. For communication, the system dynamically selects between Wi-Fi and LoRaWAN, depending on local connectivity, thus ensuring flexible deployment.

The architecture combines open-source software and off-the-shelf hardware, enhancing reproducibility and affordability.

A comparative study of multiple active infrared detectors was conducted, evaluating power consumption, detection accuracy, susceptibility to interference, and horizontal beam angle. This analysis addresses the lack of systematic evaluations of active infrared technologies for pedestrian monitoring and provides guidelines for component selection in similar systems.

The results demonstrate that the proposed system enhances both accuracy and energy efficiency, achieving up to 97% precision and a fivefold improvement in operational autonomy relative to conventional AIR-only solutions, thereby enabling reliable, real-time, and non-intrusive pedestrian monitoring.

KEYWORDS: *Infrared Sensor Comparison*, *Pedestrian Counting*, *Low-Power Sensor Networks*.

[This page has been intentionally left blank]

Contents

List of Figures

[This page has been intentionally left blank]

List of Tables

[This page has been intentionally left blank]

List of Acronyms

AIC: Akaike Information Criterion

AIR: Active Infrared

BIC: Bayesian Information Criterion

CCTV: Closed-Circuit Television

DC: Direct Current

DSRM: Design Science Research Methodology

ESP32: Espressif32

EVOA: Tagus Estuary Bird Observation and Conservation Area

GPIO: General-Purpose Input/Output

GSM: Global System for Mobile Communications

HOD: Histogram of Oriented Depths

IDE: Integrated Development Environment

IoT: Internet of Things

IR-UWB: Infrared Ultra-Wideband

KS: Kolmogorov Smirnov

LoRaWAN: Long range Wide Area Network

MQTT: Message Queuing Telemetry Transport

PIR: Passive Infrared

RGB-D: Red Green Blue-Depth

SRAM: Static Random-Access Memory

SVM: Support Vector Machine

ToF: Time-of-Flight

UML: Unified Modeling Language

CHAPTER 1

Introduction

The present chapter is concerned with the presentation of the context, technological overview, motivation and goals in this dissertation. In addition, the research questions, research method and contribution are also presented, as well as the organization of this dissertation.

This chapter is organized as follows: section 1.1 describes the context, section 1.2 provides a technological overview and section 1.3 presents the motivation of this dissertation. Then, section 1.4 defines the goals of this dissertation, section 1.5 formulates the research questions and section 1.6 describes the research method. Finally, sections 1.7 and 1.8 present the contributions and dissertation organization, respectively.

1.1. Context

Pedestrian counting and flow monitoring are critical components of urban planning, transportation management, and smart city and tourism applications. A particularly relevant context involves natural reserves and protected environments. In such contexts, meticulous management is crucial to ensure the harmonious balance between human activities and environmental conservation [1]. As illustrated by Figure 1.1, there is a need for accurate, non-intrusive monitoring solutions in cases involving sensitive natural areas that tourists frequently visit.

FIGURE 1.1. Examples of human activity in sensitive areas

In remote or environmentally sensitive areas, such as natural reserves, wildlife sanctuaries, and heritage sites, human presence must be meticulously monitored to ensure the

preservation of ecological integrity and minimize disturbance to local ecosystems. These regions frequently attract visitors for educational, recreational, or tourism purposes, making it essential to track pedestrian activity in a non-intrusive and sustainable manner. However, such environments typically lack access to stable electrical infrastructure and network connectivity, posing significant challenges for the deployment of conventional monitoring systems. The necessity for autonomous, low-power, and intermittently connected sensing solutions is therefore paramount, as they enable continuous data collection and transmission without reliance on grid power or permanent communication infrastructure.

By facilitating the acquisition of real-time data on pedestrian flow, movement direction, and speed, the system enables a comprehensive understanding of human mobility dynamics. These data-driven insights can inform and optimize operational decision-making, support proactive safety and crowd management strategies, and contribute to the long-term analysis of mobility trends and behavioral patterns in both densely populated urban areas and resource-constrained remote environments.

This research was developed as part of an ongoing collaboration between the research centers ISTAR and IT-IUL, initially within the framework of the European project RESETTING, and more recently under the scope of the national project EUROSTIT. Both initiatives aim to promote innovation in smart tourism and digital transformation through the integration of sensing, communication, and data analysis technologies. Within this collaborative context, several scientific outputs have been produced [2–4], which contribute to the broader research effort supporting the development and validation of the proposed system.

1.2. Technological overview

Many techniques exist for pedestrian counting. In the following paragraphs, we provide an overview of them.

Passive infrared sensors (PIR) detect motion by sensing variations in infrared radiation emitted by warm bodies, such as humans, moving across their field of view. It is inexpensive, energy-efficient, and privacy-compliant, but offers limited range and accuracy, and cannot reliably infer direction.

Active infrared sensors (AIR) emit infrared light and detect its reflection or interruption when a person crosses the beam. This method is slightly more accurate than PIR and can infer direction when dual beams are used, though it still has a short detection range and may be affected by ambient lighting conditions.

Pressure mats (floor sensors) detect weight or pressure changes when individuals step on the sensing surface. They are simple, robust, and unaffected by lighting conditions, but can only detect people in direct contact with the sensor and cannot distinguish individuals or determine direction effectively.

RGB cameras combined with computer vision algorithms allow for detection, tracking, and counting pedestrians in standard video feeds. This video analytics approach

offers high accuracy and rich contextual information, such as direction and density, but entails high costs, significant energy consumption, and potential privacy concerns under GDPR.

Thermal/infrared cameras detect heat signatures rather than visible light, allowing operation in low-light or night conditions while preserving privacy better than RGB cameras. However, they generally provide lower resolution and come at a moderate cost.

LiDAR and similar depth-sensing devices generate three-dimensional point clouds using laser pulses or structured light, enabling precise counting and direction detection without capturing identifiable imagery. They are accurate and privacy-friendly, though expensive and moderately power-hungry.

Radar (mmWave sensors) emit radio waves and analyze their reflections to determine movement, speed, and direction. They perform reliably under all lighting and weather conditions and offer strong privacy protection, but require complex signal processing and entail higher costs. Together with LiDAR, these are often called **Time-of-Flight (ToF)** techniques as they both measure the travel time of emitted and reflected signals, combining the accuracy of depth sensing with strong privacy protection, since they do not capture detailed images of individuals.

Wi-Fi / Bluetooth probe detection relies on signals periodically emitted by mobile devices searching for network connections. It is low-cost and capable of covering large areas without direct contact, though its accuracy depends on device density and signal variability, and some privacy concerns remain.

Mobile / cellular location data approaches use anonymized information from network operators or mobile applications to estimate pedestrian flows over large areas. While they require no on-site installation and provide broad coverage, their spatial precision is limited, and they depend on third-party data availability.

Drone-based systems capture aerial video or imagery that can be processed through computer vision algorithms to estimate pedestrian counts and movement patterns. This technique enables wide-area and dynamic monitoring but is expensive, energy-intensive, and subject to privacy and regulatory constraints.

Social Media (Crowd Signals) approaches infer pedestrian presence and density from geotagged posts, check-ins, or other digital traces on social media platforms. It is inexpensive and broad in spatial scope, yet highly imprecise, biased toward active social media users, and unsuitable for real-time pedestrian counting.

The main features of these techniques are summarized in Table 1.1. Shaded rows indicate techniques that are not simultaneously low-cost, highly GDPR-compliant, and of at least medium precision. Unshaded techniques—PIR, AIR, pressure mats, and Wi-Fi/Bluetooth probes—represent the most balanced options in terms of cost, privacy, and accuracy.

TABLE 1.1. Comparative evaluation of pedestrian counting techniques

Technique	Cost	GDPR Compliance / Privacy	Detection Range	Precision / Accuracy	Direction Detection	Energy Consumption
PIR (Passive Infrared Sensor)	Very Low	High	Low	Low–Medium	Low	Very Low
AIR (Active Infrared Sensor)	Low	High	Low	Medium	Medium	Very Low
Pressure Mats / Floor Sensors	Low	High	Very Low	Medium	Low	Low
RGB Cameras (Video Analytics)	Medium–High	Low–Medium	High	High	High	High
Thermal / Infrared Cameras	Medium	High	Medium	Medium–High	Medium	Medium
LiDAR / Depth Sensors	High	High	Medium	High	High	Medium–High
Radar / mmWave Sensors	High	Very High	Medium–High	Medium	Medium	Low
Wi-Fi/Bluetooth Probe Detection	Very Low	Medium	High	Low–Medium	Medium	Low
Mobile / Cellular Location Data	Medium–High	Medium–High	Very High	Low–Medium	Low	Very Low
Drone / Aerial Imagery	High	Low	Very High	Medium–High	High	Very High
Social Media / Crowd Signals	Very Low	Medium–High	Very High	Very Low	Low	Very Low

1.3. Motivation

As seen in the previous section, currently available pedestrian counting solutions tend to prioritize accuracy or energy efficiency, but rarely achieve both objectives simultaneously. For instance, camera and ToF-based systems offer precise measurements but require high energy and computational resources, while Passive Infrared (PIR) sensors provide low-power operation at the cost of limited precision and directional awareness [5, 6]. This imbalance highlights a persistent technological gap in the field of pedestrian monitoring.

The motivation for this research derives from the need to develop a cost-effective, low-power, and autonomous sensor system capable of operating reliably in infrastructure-limited environments. By combining PIR-based activation with AIR-based detection and integrating flexible communication interfaces such as Wi-Fi and Long range Wide Area Network (LoRaWAN), the proposed system aims to provide accurate, real-time pedestrian data while maintaining long-term energy autonomy. Its adaptable architecture enables seamless deployment across diverse operational environments, ensuring reliable connectivity under varying infrastructure conditions. This approach directly supports sustainable

tourism management, conservation planning, and the broader development of energy-efficient Internet of Things (IoT) solutions for smart and remote environments.

This work proposes a pedestrian detection system consisting of two pairs of AIR detectors arranged in parallel and two PIR detectors, one on each side of the walking path. PIRs have lower power consumption than AIRs, but lack precision. To achieve a balanced approach, the PIRs are maintained in a constant state of activity, while the AIRs and associated computational processes are activated exclusively in the presence of a human, thereby ensuring optimal energy efficiency. This critical feature in off-grid areas, where batteries must be used, does not compromise the accuracy in detecting the number of pedestrians, their speed, and direction of movement. The achievement of this objective is realized through the analysis of the AIRs activation sequence.

This work presents a system architecture intended for real-world deployment, and includes a comparative evaluation of multiple AIR detectors, analyzing their power consumption, detection accuracy, susceptibility to interference, and horizontal beam angle. It is important to note that manufacturer-provided detector specifications, when available, are typically obtained under controlled laboratory conditions that may not accurately represent the operational environment of the target system. This distinction is critical, as product datasheets frequently lack critical relevant performance details and may overstate reliability, underscoring the need for empirical testing to validate detector accuracy and consistency under realistic conditions. Consequently, this study developed an experimental setup that independently evaluates multiple AIRs owing to the necessity of a comparative analysis. This evaluation aimed to identify the most suitable components for accurate and efficient pedestrian detection in diverse real-world conditions.

1.4. Goals

The primary objective of this research initiative is to develop a precise sensor-based system that provides real-time pedestrian flow data while maintaining energy efficiency and minimizing costs by employing open-source solutions and low-cost hardware.

The main goal is composed of a series of sub-goals which, when met, will ultimately lead to its achievement:

- Develop a hybrid sensor system that integrates PIR detectors for low-power activation with AIR detectors for precise pedestrian detection.
- Achieve accurate, reliable, and real-time detection, counting, and direction tracking of pedestrians.
- Design a system architecture for extended energy autonomy and cost-effective operation in remote or infrastructure-limited environments.
- Validate the performance and robustness of the proposed architecture through deployment and testing in real-world scenarios.

1.5. Research Questions

This dissertation aims to provide answers to the research questions shown below.

- RQ1- Which AIR detector offers the optimal balance between accuracy, interference resistance, and power efficiency for integration into a pedestrian counting system?
- RQ2 - How accurately does the proposed hybrid PIR–AIR sensor count pedestrians under real-world environmental and spatial conditions?
- RQ3 - To what extent can the temporal sequence of beam interruptions be used to estimate the projected length of crossing objects?
- RQ4 - How effectively does the projected length–based calibration procedure reduce counting errors and enhance precision?
- RQ5 - What is the expected energy consumption and operational autonomy of the proposed system, and how does it compare with conventional AIR-only solutions?

1.6. Research Method

This dissertation adopts the Design Science Research Methodology (DSRM) [7], which structures the work into sequential stages of problem identification, solution design, development, evaluation, and communication.

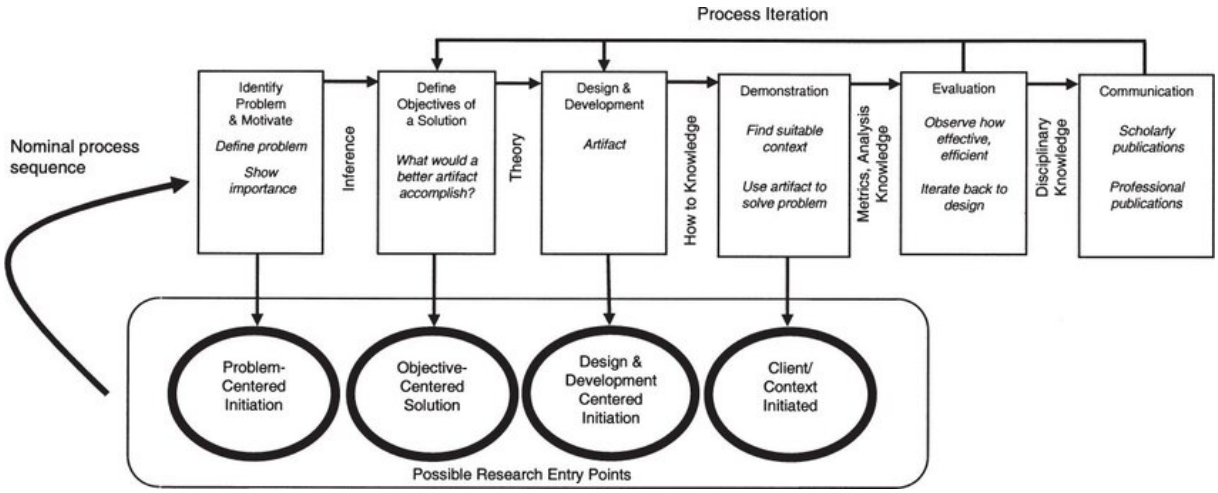

FIGURE 1.2. DSRM process model [7]

The first stage, *Problem Identification and Motivation*, is addressed in Chapter 1, which defines the research context, motivation, and objectives. It identifies the lack of energy-efficient and accurate pedestrian counting systems capable of operating in remote environments with limited infrastructure.

The second stage, *Definition of the Objectives of a Solution*, is also presented in Chapter 1, where the goals of the proposed system are outlined, including real-time monitoring, low power consumption, extended autonomy, and flexible communication through Wi-Fi and LoRaWAN.

The third stage, *Design and Development*, corresponds to Chapters 3 and 4. Chapter 3 presents the overall system architecture, including the integration of PIR and AIR detectors, while Chapter 4 details the comparative evaluation of AIR detectors under uniform testing conditions.

The fourth and fifth stage, *Demonstration and Evaluation*, is presented in Chapter 5, where field experiments were conducted to validate the system's energy efficiency, counting accuracy, and calibration process based on projected length estimation.

Finally, the sixth stage, *Communication*, is addressed in Section 6.3, which presents the dissemination of this research.

1.7. Contributions

The main contributions of this dissertation are:

(1) Development of a system capable of monitoring pedestrian movement in real time with limited infrastructure.
(2) Conducting a comparative analysis under uniform and application-relevant conditions, essential to ensure a fair and reliable assessment of detector performance.
(3) Fivefold improvement in sensor operational autonomy compared with conventional AIR-only solutions, extending its capability for long-term, battery-powered deployment.
(4) Achieved measurement accuracy of up to 97%, demonstrating high precision in pedestrian detection and counting.
(5) The application and validation of the system in real scenarios.
(6) An international conference paper and poster exhibition at ICUFN 2025, where the system architecture and AIR detectors comparison were presented [8].
(7) An international conference paper accepted for presentation at SmartIoT 2025 [4].
(8) An online asynchronous presentation at the 2025 STARS Symposium at Bridgewater State University.
(9) The source code availability of the proposed system in the GitHub repository.

1.8. Dissertation Organization

This section outlines the organization of the dissertation and provides a brief description of each chapter. Chapter 2 presents a state-of-the-art review of pedestrian detection techniques. Chapter 3 provides a comprehensive overview of the proposed system architecture. Chapter 4 focuses on the comparison and selection of the AIR detector, addressing Research Question RQ1. Chapter 5 presents the validation and performance evaluation of the proposed system, addressing Research Questions RQ2 to RQ5 through experimental analysis. Finally, Chapter 6 offers conclusions, suggestions for future work and details the dissemination efforts.

[This page has been intentionally left blank]

CHAPTER 2

Literature Review

This chapter presents the state of the art in pedestrian detection technologies, reviewing existing approaches while highlighting their advantages, limitations, and relevance to the development of the proposed low-power hybrid solution.

This chapter is organized as follows: section 2.1 reviews the main pedestrian detection technologies and academic approaches, outlining their advantages and limitations. Section 2.2 presents existing commercial solutions, while section 2.3 compares academic and commercial systems, highlighting research gaps and motivating the proposed hybrid architecture.

2.1. Pedestrian Detection Technologies

Pedestrian detection systems have been the subject of extensive research in transportation engineering [9] and smart city applications [10, 11]. Various approaches have been investigated, incorporating camera-based techniques and sensor-driven solutions, such as ToF, PIR and AIR. Each of these approaches offers distinct advantages and challenges [5, 6].

Camera-based approach:

This approach uses video and image processing techniques to extract information about objects in the captured scenes [12]. While such systems can achieve high levels of accuracy and enable advanced functionalities such as object classification, tracking, and behavior analysis [13], they also introduce several limitations [5]. Firstly, the continuous collection and processing of visual data raise significant privacy concerns, particularly in public or sensitive environments where individuals may be recorded without their explicit consent. Such practices are strictly regulated, and in many cases prohibited, within the European Union under the General Data Protection Regulation (GDPR). Secondly, video-based systems require considerable computational resources, including powerful processors and dedicated hardware accelerators, to manage the substantial volumes of image data in real time [13]. This requirement is associated with high power consumption, which renders these solutions suboptimal for battery-powered or resource-constrained deployments in remote areas. Furthermore, visual-based methods are inherently susceptible to variations in environmental conditions. For instance, performance may degrade under poor or variable lighting, during nighttime operation, or in the presence of obstructions such as fog, rain, or shadows [5], often leading to unreliable detection results. Collectively, these

challenges restrict the applicability of camera-based systems in scenarios where energy efficiency, privacy preservation, and robustness under diverse environmental conditions are critical design requirements.

In their study, the authors of [14] investigated the potential of computer vision techniques for people counting in transportation systems. The evaluation of the work focused on the use of deep learning detectors for monitoring passenger flow on metropolitan trains, achieving over 92% mean counting accuracy. The study demonstrated how existing Closed-Circuit Television (CCTV) infrastructure could be repurposed for automated people tracking and dwell-time analysis.

Spinello and Arras in [15] proposed a people detection algorithm for Red Green Blue-Depth (RGB-D) sensors that combines depth and color data to identify human silhouettes even under poor lighting conditions. The employment of Histogram of Oriented Depths (HOD) and Combo-HOD methodologies has been demonstrated to enhance the speed and reliability of robotic and surveillance applications.

ToF approach:

Alternatively, this approach technologies offer strong potential for pedestrian detection and monitoring. These systems emit laser or ultrasonic pulses and measure the time it takes for the reflected signal to return, enabling precise distance estimation and accurate 3D mapping of the environment [15]. These characteristics render them effective for tracking movement trajectories and estimating pedestrian speed, while also ensuring robustness under varying illumination conditions, including complete darkness [6]. However, it should be noted that these advantages are accompanied by significant drawbacks. ToF units continue to be comparatively costly when contrasted with alternative sensing modalities. The generation and processing of dense point-cloud data necessitate substantial energy, thereby constraining their applicability in battery-powered or off-grid configurations [5]. Furthermore, integration frequently entails an increase in system complexity, encompassing calibration, synchronization, and computational overhead for real-time processing [15]. These factors impose constraints on the implementation of large-scale or low-cost applications, despite the high accuracy that such systems can deliver.

Hnat *et al.* in [16] presented Doorjamb, an unobtrusive room-level tracking system that utilizes ultrasonic range finders mounted above doorways, pointed downward to sense people as they walk through the doorway. The system was able to estimate the direction in which the subject was walking, as well as their height, to differentiate between individuals. The system achieved 90% tracking accuracy while maintaining privacy and low cost.

Choi *et al.* in [17] developed a bidirectional people counting system based on Infrared Ultra-Wideband (IR-UWB) radar sensors. Two radar modules were positioned across a passageway to detect the order and timing of crossings, thereby enabling direction discrimination without the need for cameras. The system was subjected to a field test

in a subway station over the course of one week. This experiment resulted in an error rate that remained below 10%, even in the presence of simultaneous crossings and varying crowd densities.

PIR approach:

Another option is the use of PIRs, which detect variations in infrared radiation emitted by warm objects, such as human bodies. Upon entering the detector's field of view, a change in the thermal signature is captured and interpreted as an event [18]. This straightforward operating principle enables PIRs to function reliably without complex calibration or extensive processing requirements. PIR-based systems are particularly valued for their low power consumption and cost-effectiveness, characteristics that make them attractive for large-scale deployments and battery-powered applications where energy efficiency is a critical constraint [5]. In practice, PIRs have therefore been widely adopted in contexts such as occupancy detection, automated lighting, and basic security systems [19]. But these detectors are also highly susceptible to environmental factors, including temperature fluctuations and sunlight interference [6]. These constraints render PIRs particularly well-suited for simple presence detection as opposed to accurate, directional pedestrian flow monitoring and counting.

A low-cost PIR sensor array installed above doorways for indoor occupancy estimation is proposed in [20]. The design incorporated an unsupervised pattern-recognition algorithm and the Z-Wave protocol for data transmission. The system was able to ensure the confidentiality of visual data, thereby preserving the privacy of the subjects under investigation. Furthermore, it demonstrated a high level of accuracy when operating in typical indoor conditions.

PIR detectors have been utilized for the purposes of motion detection, with ZigBee or Wi-Fi modules being used for cloud integration. For instance, [18] were responsible for the development of a PIR-based intrusion detection system that demonstrated the feasibility of using low-cost, low-power wireless sensor networks for security purposes.

An IoT-enabled pedestrian counting and environmental monitoring system designed for smart city applications is presented in [11]. The prototype incorporated PIR motion detectors for pedestrian detection, along with temperature, humidity, and CO_2 sensors. These sensors were connected through a Wi-Fi network to an online dashboard, enabling real-time visualization. The system facilitated low-cost data acquisition for both pedestrian traffic analysis and environmental quality assessment, thereby demonstrating reliable cloud integration and scalability for urban deployments. Consequently, this initiative gave rise to the Melbourne Pedestrian Counting System, an automated network comprising over 80 sensors strategically positioned throughout the city to facilitate the

real-time collection of pedestrian flow information. This system has been designed to optimize the decision-making process and facilitate the development of future urban planning initiatives.

AIR approach:

AIR detectors operate by emitting an infrared beam that is interrupted when an object passes through, making them highly suitable for pedestrian counting. They exhibit substantially reduced energy consumption compared to camera-based systems and ToF, making them more suitable for battery-powered applications. However, their consumption remains higher than that of PIRs [5, 6]. Furthermore, they are small and affordable, and since they do not capture images or personal data, they do not infringe on privacy regulations.

AIRs also have limitations, particularly in scenarios with groups of pedestrians. In addressing these limitations, research efforts have been directed toward reducing the discrepancy between the ground truth and the detector counts. The tendency of sensors, supported by AIRs, to underestimate the number of pedestrians, a phenomenon particularly pronounced when individuals walk side by side or in groups, was analyzed in [21]. The authors proposed a non-parametric statistical calibration method that utilizes bivariate bootstrap sampling to address this issue. This approach seeks to adjust the raw detector data to more accurately reflect the actual number of pedestrians, thereby enhancing the data quality.

The enhancement of counting precision by analyzing time-continuous data from AIRs is discussed in [22]. The authors developed a people-counting model based on Support Vector Machine (SVM) algorithms. This model effectively distinguished individual pedestrians, even when multiple people simultaneously passed through the detector's detection area, improving counting accuracy compared to previous approaches.

A bi-directional portable people counter based on the IoT is proposed in [23]. The counter is equipped with two AIR detectors and a microcontroller with Global System for Mobile Communications (GSM) capabilities, which facilitates GSM-based cloud communication. The system attained an average accuracy of 97.33%, and its design was intended for environments with a single entrance/exit.

Given the trade-offs identified in the literature, an optimal pedestrian counting solution should leverage the high accuracy of AIR detectors while mitigating the energy consumption associated with continuous sensing, data processing, and wireless communication. Although PIR sensors are less precise, they offer a critical advantage for low-power operation, as they can activate the sensing system only when motion is detected. This selective activation significantly reduces standby power consumption, thereby extending the operational autonomy of battery-powered installations.

Building on this rationale, the present research proposes a hybrid architecture in which a PIR detector triggers the activation of AIR detectors and the processing unit, coupled with a flexible network deployment for uplink communication. This motion-triggered design enables efficient energy utilization without compromising detection performance.

2.2. Commercial Solutions

Concurrent with academic research, the development of commercial solutions has emerged as a facilitating factor in the monitoring of pedestrians and occupancy. The solutions above serve to bridge the gap between experimental sensing approaches and real-world deployment by providing scalable, networked, and data-driven tools for urban mobility analysis, retail analytics, and environmental optimization.

Eco-Counter offers a comprehensive range of outdoor pedestrian and cyclist counting systems, employing technologies such as camera and PIR-based detectors. These systems are suitable for both temporary and permanent installations, enabling continuous data collection at six-hour intervals via 4G/LTE connectivity, even under diverse environmental conditions. The company's proprietary data analytics platform supports automated aggregation, visualization, and reporting of long-term mobility trends, providing valuable insights for urban planning, transportation management, and tourism development.

SensMax provides wireless people-counting solutions that employ cameras and AIR detectors with Wi-Fi or 4G/LTE connectivity, targeting both retail environments and public spaces. The systems are designed for simple installation and maintenance, offering a scalable architecture suitable for multi-site deployments. Sensor prices vary between 265€ and 1200€, depending on the model and configuration.

WeCountPeople offers a suite of PIR, AIR, and camera people-counting solutions developed for diverse applications, including crowd management, retail analytics, and smart building monitoring. The company's systems feature bidirectional detection, ensuring reliable operation in both indoor and outdoor environments. Sensor prices vary between $129 and $699, depending on the model and configuration.

2.3. Discussion

Table 2.1 provides an overview of the main academic projects and commercial products related to pedestrian detection and people-counting systems. It summarizes key aspects, including the sensing technologies employed, communication methods, autonomy, reported errors, and intended target locations for each solution.

A comparative analysis of existing academic and commercial solutions reveals that none simultaneously address the challenges of real-time communication, battery-powered operation, low counting error, and applicability to both indoor and outdoor environments. Most current systems are either limited to indoor settings or require a continuous external power supply to operate effectively. Furthermore, achieving high precision often entails increased energy consumption or complex installation procedures. Within this

TABLE 2.1. Related works (top) and commercial solutions (bottom)

Project	**Technology**	**Communic.**	**Autonomy**	**Error**	**Target Location**
Sirikham et al. [23]	AIR	GSM	NA	2.67%	Indoor (Single entrance/exit)
Perra et al. [20]	PIR	Z-Wave	NA	5%	Indoor (Doorway)
Hnat et al. [16]	ToF	NA	NA	10%	Indoor (Doorway)
Velastin et al. [14]	Camera	NA	NA	8%	Indoor/Outdoor (Public Transport)
Spinello et al. [15]	Camera	NA	NA	15%	Indoor
Choi et al. [17]	ToF	NA	NA	10%	Indoor
Sahoo et al. [18]	PIR	ZigBee	NA	NA	Indoor
Akhter et al. [11]	PIR	LoRaWAN	Solar Panel	10%	Outdoor
Eco-Counter	PIR/Camera	4G/LTE	2-year	NA	Indoor/Outdoor
SensMax	AIR/Camera	Wi-Fi/4G	NA	Down to 1%	Indoor/Outdoor
WeCountPeople	PIR/AIR/Camera	NA	Up to 1-year	7%	Indoor/Outdoor

NA: Not Available

context, the proposed hybrid PIR–AIR pedestrian counting system represents a notable advancement in the state of the art, as it combines energy efficiency, real-time wireless communication, and reliable performance. This integration of capabilities — absent in previous approaches — highlights the practical contribution and innovative character of the developed solution to the field of low-power pedestrian monitoring.

CHAPTER 3

System Architecture

This chapter delineates the architecture and technologies employed in the proposed system. The chapter is organized as follows: section 3.1 presents the architecture for the proposed system, section 3.2 details the methodology used for projected length estimation, section 3.3 describes the technologies adopted for its implementation, and section 3.4 introduces the developed sensor prototype.

3.1. Proposed system architecture

The system must be designed to continuously monitor and analyze pedestrian movement within the designated zone, providing accurate, real-time, and contextually relevant information to interested parties.

The main requirements of the proposed system architecture are as follows:

- The use of PIR detectors to activate the system, enabling energy-efficient operation;
- Flexible communication capabilities, allowing data transmission through multiple network interfaces.

The first requirement focuses on system activation by PIR sensors. The proposed system architecture is supported by insights from the preceding literature, integrating low-power PIR detectors that activate the AIR higher power sensing, processing, and communication units exclusively upon detection of motion. In Figure 3.1, the operating principle of the proposed hybrid pedestrian detection sensor is illustrated.

Two PIR detectors are positioned at the outer extremities of the configuration, with each detector oriented towards one of the two possible walking directions along the pathway. This ensures continuous monitoring for motion within their respective fields of view. Upon detection of motion by one of the PIRs, the system triggers the activation of the remaining components, including the two pairs of AIR detectors. Each pair consists of a transmitter (Tx) and a receiver (Rx) that are aligned across the designated passageway. As a pedestrian traverses the area, the interruptions of the two AIR infrared beams are detected and used to register the movement. By analyzing the chronological sequence in which these beams are interrupted, the system determines the pedestrian's direction of movement. Furthermore, as elaborated in Section 3.2, the temporal relationships between beam interruptions are subsequently employed to estimate the projected length of the detected object, thereby enhancing the discrimination between single and multiple crossings.

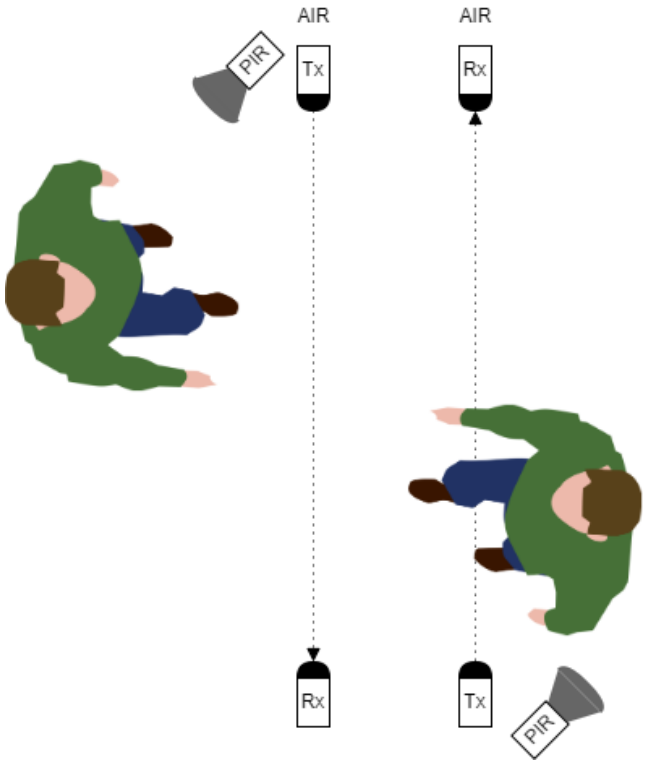

FIGURE 3.1. Working principle of the hybrid PIR–AIR pedestrian detection system

This design choice minimizes energy consumption during inactive periods, thereby enhancing the system's overall efficiency and operational autonomy under battery-powered or resource-constrained conditions. This feature is particularly advantageous in environments with low pedestrian traffic, where infrequent activity enables the sensors to remain in extended sleep states. This ensures reliable long-term operation with minimal maintenance or recharging requirements.

The second requirement focuses on communication flexibility. The implementation of a versatile communication approach, previously validated by this research team [24], ensures reliable data transmission across diverse network conditions while maintaining adaptability to different deployment contexts. The system guarantees uninterrupted data transmission through its ability to select the most suitable communication interface based on connectivity availability. This strategy enhances robustness and scalability while reinforcing the practicality of the solution for diverse operational scenarios, ranging from dense urban environments within smart-city infrastructures to isolated or remote areas with limited communication coverage.

The proposed architecture, illustrated in Figure 3.2, builds upon a modular framework co-developed in [4], which shares common design principles, where the sensor is configured to record the number of pedestrians that traverse it in each direction and periodically transmit this information to a cloud server.

The implementation of the proposed system relies on two core components: *PIR-Detector* and *AIR-Detector*. These modules operate in conjunction to combine the low

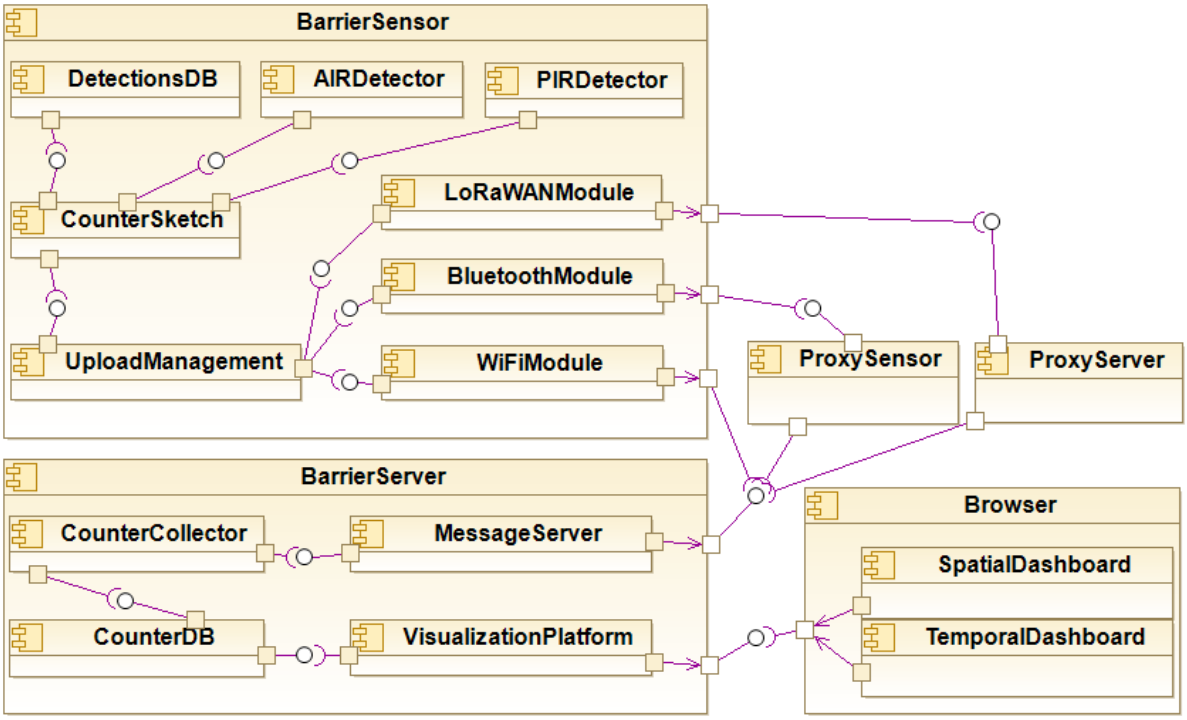

FIGURE 3.2. UML component diagram of the proposed system

power consumption characteristic of PIR sensors with the higher detection accuracy of AIR sensors. Data collected by the sensor are transmitted through multiple communication protocols, including Wi-Fi, LoRaWAN, and Bluetooth. This functionality is managed by the *Upload-Management* component, which dynamically selects the most suitable communication channel available at a given time. The resulting multi-channel capability enhances the system's adaptability to diverse deployment scenarios, ensuring reliable data transmission even in environments with limited connectivity.

The transmitted information consists of simple pedestrian counts and movement patterns, resulting in a very low data payload and eliminating the need for high-bandwidth communication. Consequently, the system operates efficiently with low-power, long-range protocols such as LoRaWAN, making it particularly suitable for remote or off-grid locations where conventional connectivity options like Wi-Fi are unavailable. This design choice significantly broadens the range of potential deployment contexts for the proposed sensor system.

The cloud server facilitates visualization of temporal and geographic data, thereby enabling a comprehensive understanding of pedestrian movements. The components that enable this functionality are the *CounterCollector* and *MessageServer*. The latter is the single entry point for all messages in the cloud server, regardless of the communication protocol used to upload the pedestrian information, ensuring transparency.

3.2. Projected Length Estimation

Accurate pedestrian detection depends not only on the reliability of the sensing hardware but also on the intelligent interpretation of the timing patterns generated during each crossing event. To enhance detection precision, this section explores a temporal analysis method based on the activation sequence of the AIR detectors. By capturing the chronological order and duration of beam interruptions, the detectors enable the analysis of temporal patterns that allow the identification of valid crossings, the filtering of false detections, and improved distinction of overlapping passages. This time-based approach forms the foundation for projected length estimation [25], which improves the sensor's ability to differentiate between single and grouped pedestrians, thereby enhancing overall counting accuracy.

The projected length of a crossing object is estimated from the timing disparities between the blocking and clearing events of the two beams. These temporal parameters are used to derive the front and rear velocities as the object passes through the detection zone, allowing the system to compute the effective length, as illustrated in Figure 3.3, which details a complete activation cycle of the AIR detectors.

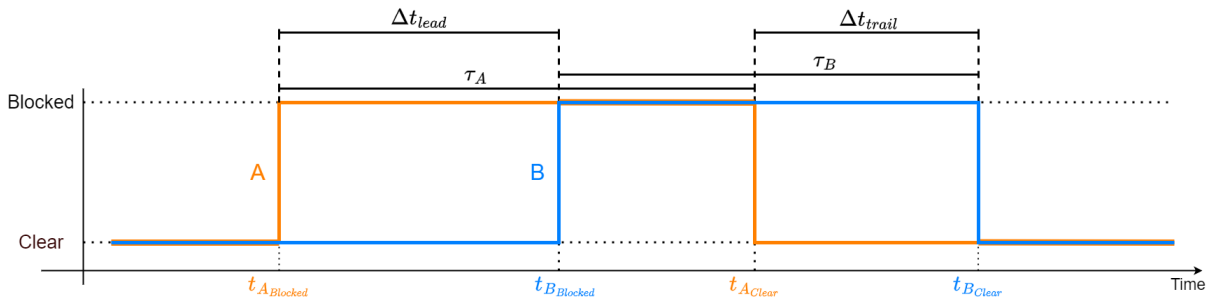

FIGURE 3.3. Activation sequence of AIR detectors A and B

By analyzing the temporal patterns associated with the blocking ($t_{Blocked}$) and clearing (t_{Clear}) of AIR detectors beams, it is possible to estimate the projected length (L) of an object as it crosses the sensor.

It is possible to ascertain the velocity of the object's front (v_{front}) and rear (v_{rear}) as it passes the detectors due to the spacing between (s) the AIRs and the time difference between blocked and clear signals. This calculation is outlined using Equations 3.1 and 3.2, respectively.

$$v_{front} = \frac{s}{\Delta t_{lead}} \tag{3.1}$$

$$v_{rear} = \frac{s}{\Delta t_{trail}} \tag{3.2}$$

By averaging the speeds (v_{avg}), previous calculated, with Equation 3.3, and the time that the detectors' beams remain blocked (τ), is possible to obtain an approximate projected length (L), with Equation 3.4.

$$v_{avg} = \frac{v_{front} + v_{rear}}{2} \tag{3.3}$$

$$L \approx v_{avg} \cdot \frac{\tau_A + \tau_B}{2} \tag{3.4}$$

These equations assume that the pedestrian moves at approximately constant speed while traversing the detection zone, an assumption that holds for most walking scenarios.

The estimation of the projected length thus provides an additional layer of information that enhances the system's ability to interpret pedestrian movement. Beyond enhancing the precision of measurement, this parameter contributes to the classification of crossings by correlating the measured length to characteristic patterns observed during single and multiple detections. The integration of temporal dynamics into spatial analysis is a critical step in enhancing the robustness of the sensing mechanism.

3.3. Adopted Technologies

The proposed system is developed using open-source software technologies and commercial off-the-shelf, low-cost hardware components, ensuring affordability, accessibility, and ease of replication.

As illustrated in Figure 3.4, an Unified Modeling Language (UML) Deployment Diagram provides a comprehensive overview of the system, representing the physical instantiation of the logical architecture defined in the UML Component Diagram (Figure 3.2). The model illustrates the interplay among hardware modules, communication layers, emphasizing the contributions of each component to data acquisition, processing, and transmission within the broader system framework.

For the computing unit of our sensors, we have opted for the Heltec Wireless Stick. The selection of this device was motivated by its compact integration of Wi-Fi, LoRaWAN, and Bluetooth communication, combined with the processing capability of the Espressif32 (ESP32) chip and the convenience of an embedded OLED display.

The local database utilizes an SQLite μLogger, which can log data into SQLite databases, even when the Static Random-Access Memory (SRAM) is as low as 2 kilobytes. It should be noted that, although data are currently stored in volatile memory variables, the implementation of a local database is planned for future versions.

The architecture of the server-side of the system was implemented using the architecture outlined by [24]. For receiving all messages, our cloud server uses the Mosquitto Message Queuing Telemetry Transport (MQTT) server, a lightweight message broker that implements the MQTT protocol, using a publish/subscribe model. This provides transparency since all messages are received in the *BarrierServer* via the MQTT protocol,

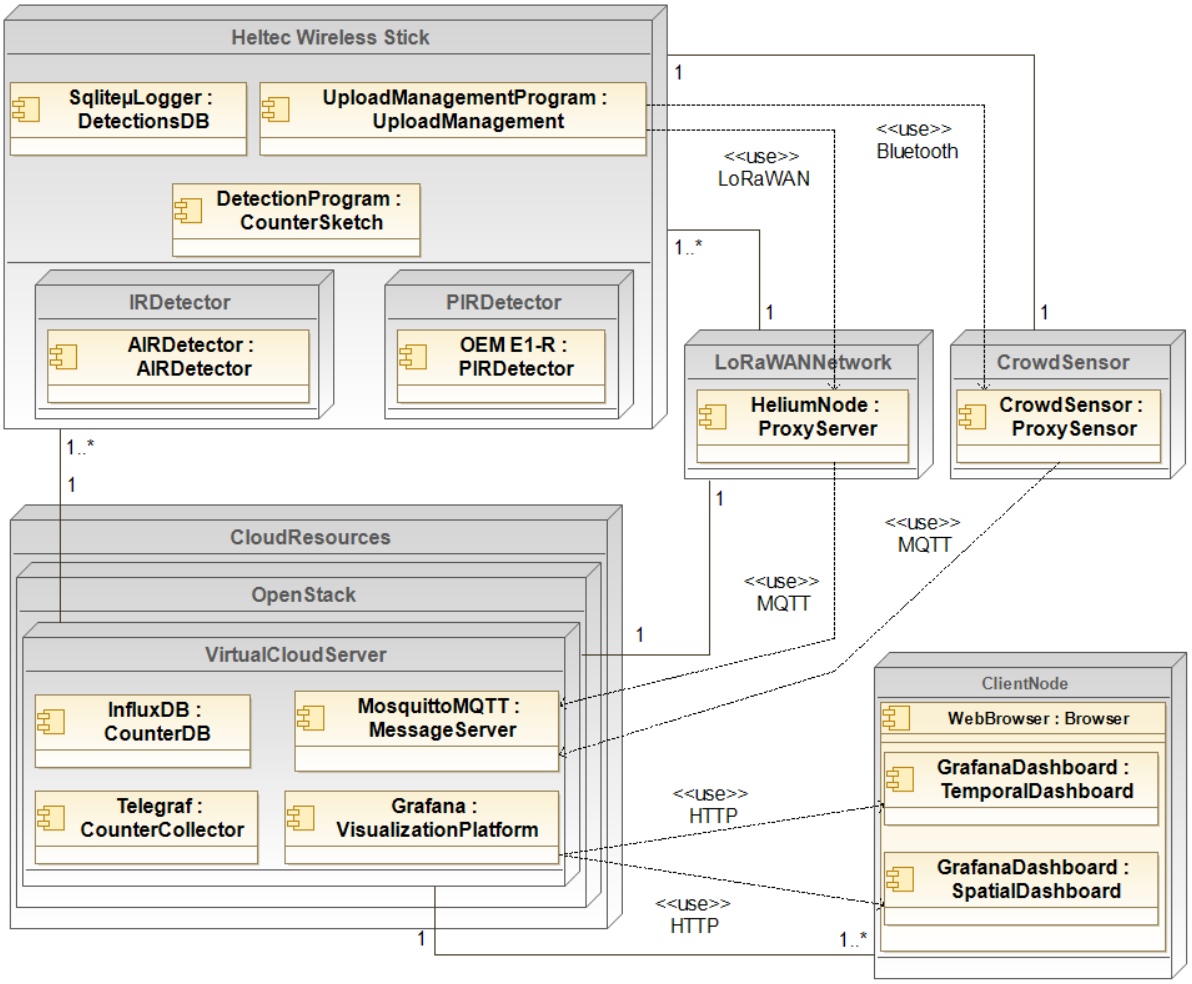

FIGURE 3.4. UML deployment diagram of proposed system

independently of the communication technology used to upload the crowding information.

For sensor data ingestion InfluxDB was chosen as a time-series database widely adopted for operations monitoring, application metrics, IoT sensor data, and real-time analytics.

For the *CounterCollector*, responsible for pushing all messages received in the *MessageServer* via MQTT protocol to the *CounterDB* in the appropriate format, we chose Telegraf, an open-source plugin-driven server agent for collecting and reporting metrics from databases, systems, and IoT sensors.

Finally, for data visualization, we chose Grafana, an open-source analytics and monitoring tool compatible with several databases, including InfluxDB. This framework can create custom dashboards with graphs and panels for viewing crowding information with different spatiotemporal granularity levels, as illustrated in Figure 3.5.

Each sensor's microcontroller not only processes the signals acquired from the detectors, but also transmits the resulting data to a cloud server using Wi-Fi, LoRaWAN, or Bluetooth communication (the Bluetooth upload feature was not implemented). When Wi-Fi connectivity is available, data are sent directly to the *MessageServer* through the

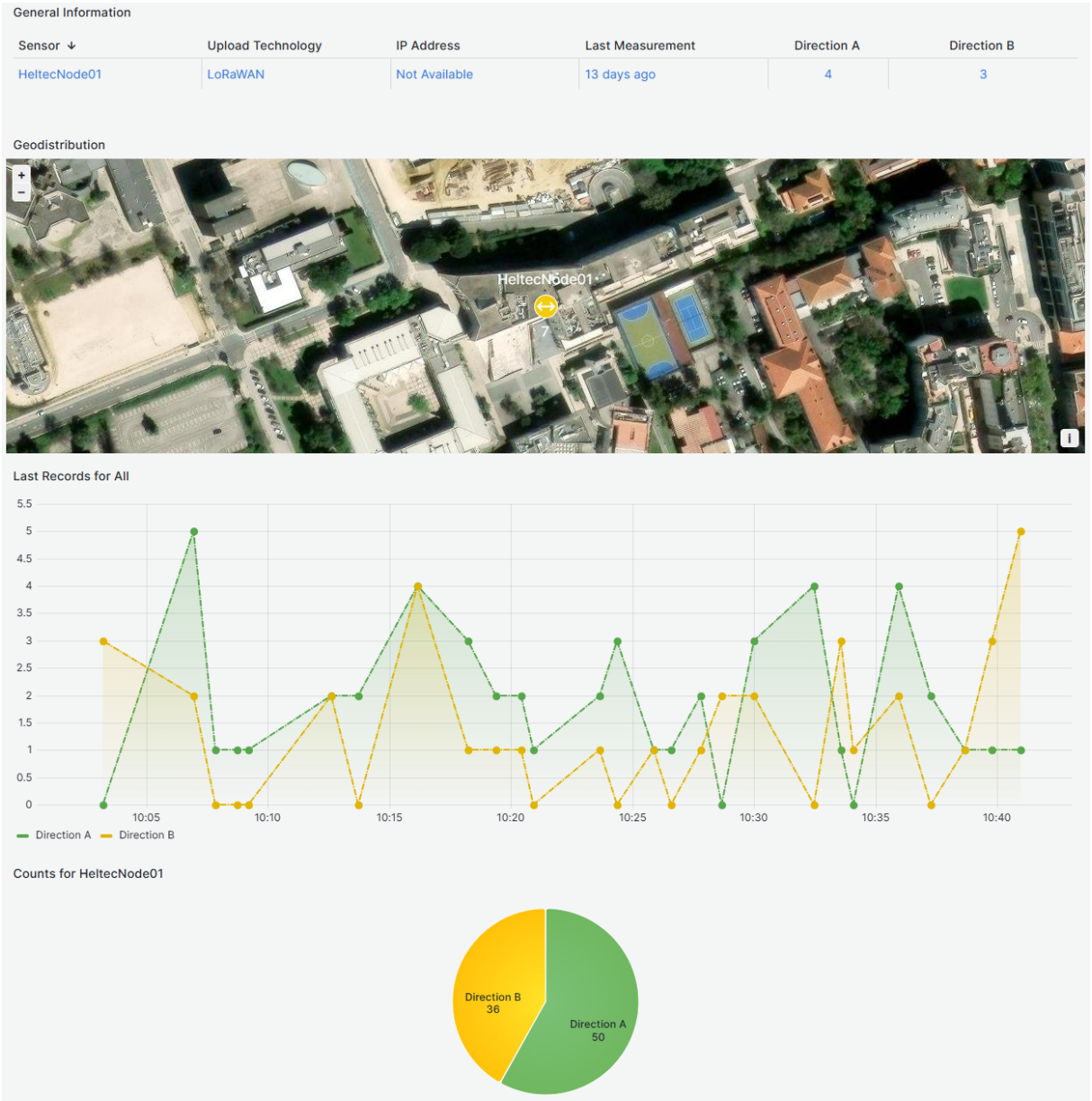

FIGURE 3.5. Grafana dashboard

MQTT protocol. In areas with limited or no Wi-Fi coverage, the system instead utilizes LoRaWAN to forward the data to a gateway, represented as the *ProxyServer* in Figure 3.2, through accessible networks such as The Things Network or Helium. Bluetooth communication could also be employed as a last-resort data upload method, enabling the transmission of information to nearby Bluetooth-capable devices, represented in Figure 3.2 as *ProxySensor*, with a potential wired internet connection. This approach would provide an additional layer of redundancy, ensuring data delivery even in scenarios where both Wi-Fi and LoRaWAN connectivity were unavailable.

The corresponding implementation details are illustrated in Figures 3.6 and 3.7, which present the breadboard layout and the complete schematic diagram of the sensor system, respectively.

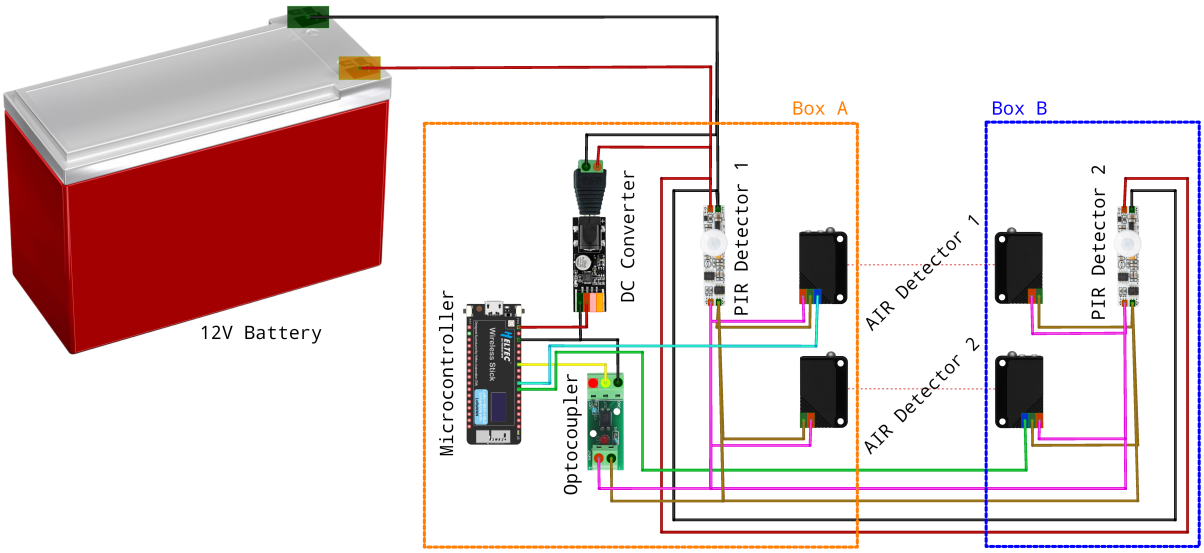

FIGURE 3.6. Breadboard diagram of sensors

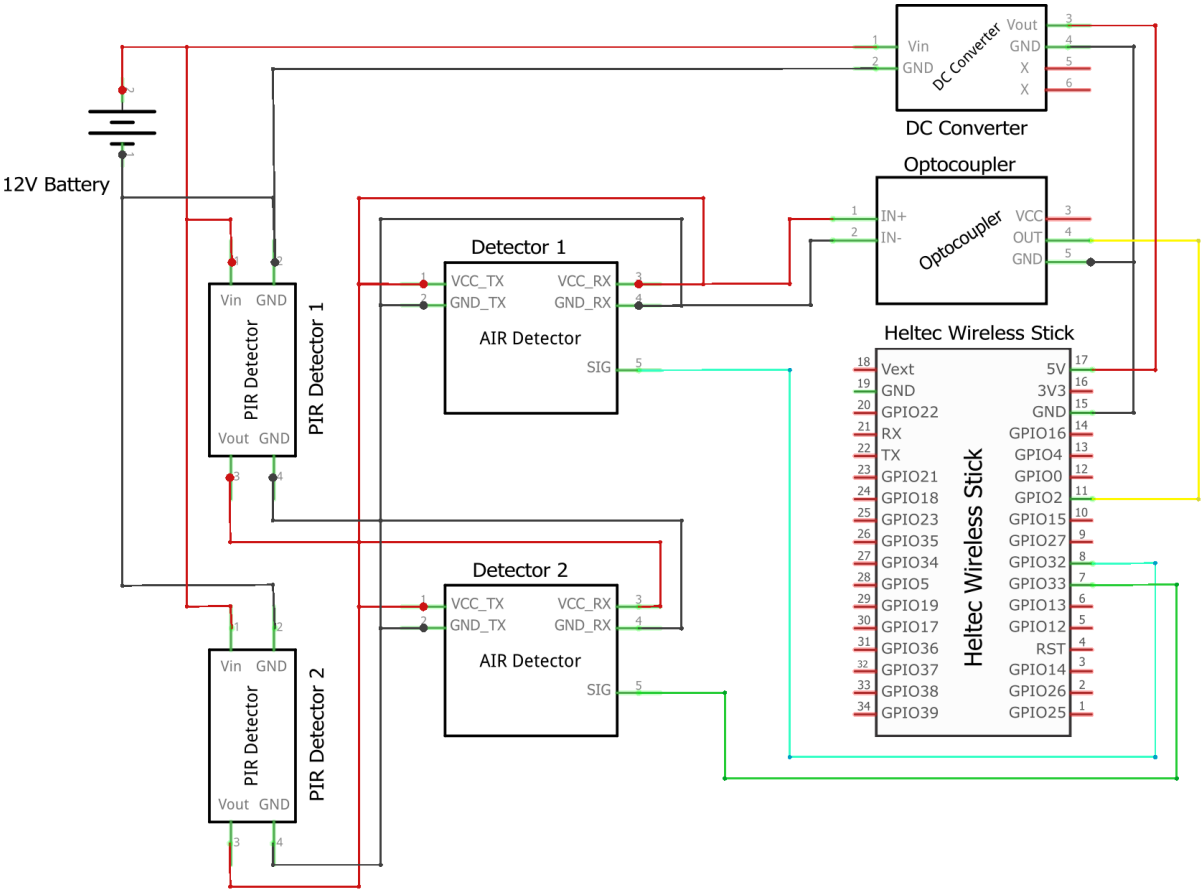

FIGURE 3.7. Schematic diagram of sensors

Each barrier sensor is equipped with two PIR detectors that, upon detecting motion, activate the AIR detectors and wake the microcontroller from its low-power state. The PIR Sensor Switch E1-R was selected for its compact, profile-mount design, which facilitates seamless integration within the sensor enclosure, and for its suitable motion detection characteristics (approximately 120° field of view and up to 3 m sensitivity).

In addition, the module's wide operating temperature range (-30 °C to 55 °C) ensures reliable performance in outdoor environments. These detectors effectively transition the microcontroller from a low-power state and activate a pair of AIRs, chosen in chapter 4.

The signals from the PIR detectors are received by the microcontroller through an optocoupler, which provides galvanic isolation to ensure reliable operation.

A 12-volt battery powers all components and requires Direct Current (DC) power-down converters since the microcontroller uses 5 volts, including on its General-Purpose Input/Output (GPIO) pins.

The sensor system is organized into two separate enclosures, referred to as Box A and Box B in Figure 3.6. Box A contains the microcontroller, one PIR detector, one AIR detector pair, a DC converter, and an optocoupler. Box B includes the remaining PIR detector and AIR detector pair. The 12-volt battery is positioned externally to the enclosures due to its larger size and ease of replacement.

The system firmware was developed using the Arduino Integrated Development Environment (IDE), selected for its open-source accessibility, extensive library support, and compatibility with the Heltec Wireless Stick microcontroller. Programming was carried out in C/C++, the primary language supported by the Arduino framework, which enables low-level hardware interaction alongside simplified high-level functions. After compilation, the program is flashed onto the microcontroller via a USB connection, using the Arduino IDE's built-in upload tool, which interfaces with the board's serial bootloader to transfer and store the binary executable in non-volatile memory.

The source code was evaluated using the SonarQube Cloud platform (Figure 3.8) to assess code quality, maintainability, and reliability, ensuring adherence to good software engineering practices. The result confirmed full compliance with good software engineering practices.

The firmware, available in open access at GitHub, is responsible for executing the pedestrian counting logic on the microcontroller.

It continuously monitors the digital inputs (GPIO7 and GPIO8) connected to the AIR detectors, visible in Figure 3.7. When a pedestrian sequentially interrupts both infrared beams, the firmware detects the event, determines the direction of movement from the order of beam activations, and increments the corresponding directional count variable. To optimize energy efficiency, the system operates in a low-power deep-sleep mode during periods of inactivity. Reactivation occurs automatically when motion is detected by the PIR detectors connected to GPIO11 of the microcontroller.

3.4. Sensor Prototype

A functional sensor prototype was designed and assembled to enable the testing and validation of the proposed system.

The sensor enclosure, presented in Figure 3.9 was designed and fabricated by Vitrivius Fablab, an architecture lab located at Iscte.

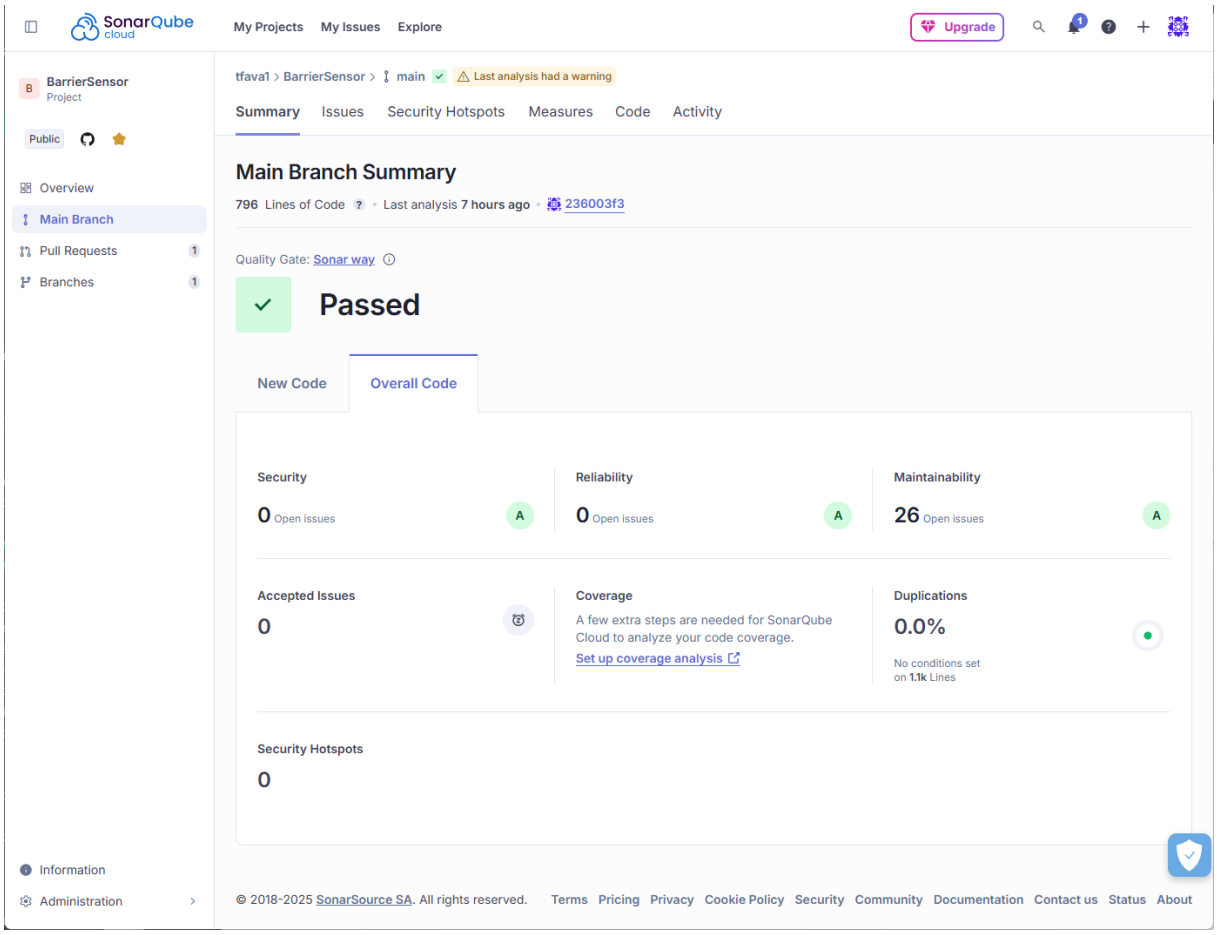

FIGURE 3.8. SonarQube Cloud analysis results of the developed source code

The developed enclosure was designed to protect the internal electronic components while ensuring accessibility for assembly and maintenance. Its internal structure provides dedicated mounting areas for the microcontroller, detectors, and panel connectors, while maintaining compact dimensions suitable for outdoor installation.

The AIR detectors were positioned 15 cm apart, exceeding the 12 cm minimum separation identified for the selected AIR detector in the detector arrangement and interference assessment (Section 4.3). This spacing ensures reliable operation by preventing mutual interference between transmitters and receivers.

In addition, the enclosures includes a 2-pin panel connector for battery connection and a 5-pin panel connector that enables power and signal interconnection between the two enclosures, facilitating modular deployment and simplified maintenance.

Table 3.1 presents the cost breakdown of the components used in the sensor prototype, including the microcontroller, sensors, connectors, battery, and 3D-printed enclosure.

The total cost of 213.15 € demonstrates the feasibility of implementing an energy-efficient and connected pedestrian counting unit at a relatively low price. The design prioritizes affordability without compromising functionality or robustness, making the

FIGURE 3.9. Overview of the developed sensor enclosure prototype: (1) microcontroller, (2) microcontroller LoRaWAN antenna, (3) AIR, (4) PIR, (5) panel connector 2 PIN, (6) panel connector 5 PIN, (7) panel micro USB adapter

TABLE 3.1. Sensor total price

Component	Quantity	Unit Price [€]	Cost [€]
Microcontroller Heltec Wireless Stick	1	21.60	21.60
AIR Detector	2	25.97	51.94
PIR Detector	2	8.92	17.84
DC Converter	1	5.30	5.30
Optocoupler	1	3.50	3.50
Eletrical cable 5 cores	1	9.80	9.80
Eletrical cable 2 cores	1	4.40	4.40
Panel Connector SP13 female 2 Pin	1	7.58	7.58
Connector SP13 male 2 Pin	1	7.04	7.04
Panel Connector SP13 female 5 Pin	2	6.00	12.00
Connector SP13 male 5 Pin	2	6.00	12.00
Panel Micro USB adapter	1	10.86	10.86
12-volt Battery	1	16.99	16.99
3D-Printed Enclosure	1	32.50	32.50
		Grand Total	213.15

solution suitable for scalable deployment in multiple locations. The use of 3D-printed enclosures further contributes to cost reduction and adaptability, allowing easy adjustments for different sensor configurations.

CHAPTER 4

Detector Evaluation and Selection

The architecture of the proposed optimized wireless pedestrian counting sensor integrates AIR sensing, data processing, and communication modules, with system activation triggered by a low-power, resource-efficient, yet less accurate PIR sensor. While AIR detectors are essential to achieving high detection accuracy, this advantage typically comes at the expense of increased power consumption. Therefore, the careful selection of an appropriate AIR detector is crucial to balance performance and energy efficiency. Through this analysis, the chapter addresses Research Question RQ1, which investigates which AIR detector offers the optimal balance between accuracy, interference resistance, and energy efficiency for integration into the proposed hybrid pedestrian counting system. To this end, six candidate AIR detectors were shortlisted for evaluation, as presented in Table 4.1.

TABLE 4.1. Active infrared detectors

ID	Detector	Type	# Freq. Ch.	Cost [€]
1	Single Beam AIR Detector - ABO-20F	Thru-Beam	4	11.10
2	Single Beam AIR Detector - ABO-20L	Thru-Beam	1	12.30
3	Acogedor E3Z-T61	Thru-Beam	1	25.97
4	STBTECH E3Z-R61	Retroreflective	1	18.24
5	DFRobot SEN0523	Thru-Beam	1	14.70
6	Irfora E3F-20C1	Thru-Beam	1	24.09

The initial selection was guided by key criteria: cost-effectiveness to support scalable deployment, commercial availability to facilitate procurement, and hardware compatibility to enable seamless integration into the system architecture.

It is important to note that manufacturer-provided detector specifications, when available, are typically obtained under differing test conditions, which may not reflect the operational context of the target system. Therefore, conducting a comparative analysis under uniform and application-relevant conditions is essential to ensure a fair and reliable assessment of detector performance. For instance, power consumption is critical in battery-powered systems, as it directly impacts operational autonomy.

Additionally, high detection accuracy and resistance to signal interference are equally important, given that the system relies on paired, parallel detector configurations to determine the direction of pedestrian movement. In such arrangements, signal overlap between adjacent detectors can result in false detections and compromise overall sensor reliability. Moreover, variations in the horizontal beam angle caused by detector misalignment or installation inconsistencies can further affect detection performance.

As such, a rigorous evaluation of the candidates was conducted to identify the most suitable detector for integration. This process involved a systematic analysis of critical parameters influencing detector performance and reliability within the intended application domain, with a particular focus on four key metrics: power consumption, detection accuracy, mutual interference under close-proximity conditions, and susceptibility to variations in horizontal beam angle. Accordingly, a structured comparison of these factors is presented in the following subsections.

4.1. Power Consumption Analysis and Optimization Strategy

In low-power systems, minimizing the energy consumption of the employed components is essential to extend operational lifespan. Table 4.2 presents each candidate detector's measured power consumption values.

TABLE 4.2. Power consumption of AIR detectors

Detector ID	Operating Voltage [V]	Power Consumption [mW]					Daily Consumption [Wh/day]	
		Transmitter (Tx)	Receiver (Rx)		Total (Tx + Rx)		1% Time Interrupted	0.1% Time Interrupted
			Uninterrupted	Interrupted	Uninterrupted	Interrupted		
1	12	219.48	77.88	276.00	297.36	495.48	7.18	7.14
2	12	215.52	53.28	255.60	268.80	471.12	6.50	6.46
3	12	32.28	17.40	59.16	49.68	91.44	1.20	1.19
4	12	NA	57.24	97.68	57.24	97.68	1.38	1.37
5	5	65.70	22.45	22.75	88.15	88.45	2.12	2.12
6	12	18.72	13.44	52.08	32.16	70.80	0.78	0.77

NA: Not Available

The energy performance of each detector was evaluated by measuring its power consumption under two operating conditions: uninterrupted (normal beam transmission) and interrupted (beam blockage). For each detector, both the transmitter (Tx) and receiver (Rx) currents were measured independently and subsequently multiplied by their respective operating voltages (indicated in the table 4.2) to obtain the power values. Furthermore, the daily energy consumption was estimated for duty cycles of 1% and 0.1%, corresponding to operating conditions where the infrared beam is occasionally interrupted by pedestrian movement. These measurements provide a comparative basis for assessing the suitability of each detector in terms of energy efficiency and long-term battery operation.

The results indicate that Detectors 1 and 2 exhibit significantly higher power consumption than the remaining candidates. This elevated energy demand would considerably shorten battery life, making these detectors less suitable for long-term, autonomous deployments. In contrast, Detectors 3, 4, 5, and 6 demonstrate substantially lower power requirements, thereby offering more significant potential for energy-efficient integration and extended system autonomy.

To reflect more realistic usage scenarios, the daily energy consumption was estimated. Detector 6 emerges as the most energy-efficient option, with approximately one order of magnitude lower daily consumption than that of the highest-consuming detector. Detectors 3, 4, and 5 also show favorable performance in terms of energy efficiency.

To illustrate the energy impact that a hybrid PIR-AIR solution imposes, the Table 4.3 shows the daily power consumption of other components of the sensor.

TABLE 4.3. Other components consumption

Component	Operating Voltage [V]	Energy Consumption [mW]	Daily Energy Consumption [Wh/day]
Microcontroller	5	343	8.23
PIR Detector	12	45.12	1.08

The integration of PIR detectors to activate both the microcontroller and the AIR detectors improves energy efficiency considerably. As demonstrated by the daily energy consumption values, the most efficient AIR (Detector 6), operating at a 1% duty cycle, consumes approximately 0.78 Wh/day, while the microcontroller requires 8.23 Wh/day when continuously active. In contrast, the power consumption of a PIR detector is 1.08 Wh/day, which is substantially lower than the power draw of the microcontroller. By maintaining the PIR in continuous operation and using it to trigger the activation of the AIR sensors and processing unit only when motion is detected, the system minimizes unnecessary energy expenditure during periods of inactivity.

This strategy facilitates an order-of-magnitude reduction in average power consumption, thereby extending battery life and enhancing the feasibility of long-term, off-grid operation without compromising detection reliability.

4.2. Detector Accuracy Evaluation

An experimental setup was designed to evaluate the accuracy of the candidate detectors in detecting motion events. The setup consisted of a test rig incorporating a DC motor with an encoder to pull a wheeled cart along a guided rail. The rail was positioned at a 5^{o} inclination to promote consistent and controlled forward motion of the cart, allowing gravity to assist in maintaining a smooth and uniform trajectory along the track. The transmitter and receiver units of the detectors were mounted 140 cm apart and perpendicular to the track, such that the passing cart interrupted the infrared beam, mimicking pedestrian motion.

The DC motor encoder enabled the cart to move at a controlled and constant speed, ensuring repeatable and precise test conditions. During each trial, the cart's motion at the detector's position was recorded using a high-speed camera configured to capture video at 240 frames/s. This allowed accurate measurement of beam interruption duration as a reference to compare against values registered by each detector.

Tests were conducted at seven distinct speeds (0.32, 0.4, 0.59, 0.78, 0.97, 1.14 and 1.34 m/s), with each speed tested five times to evaluate detector accuracy under realistic conditions, including pedestrian walking speeds reported in [26]. The experimental setup is illustrated in Figure 4.1.

Figure 4.2 also presents each detector's average relative error as a speed function. Detector 1 showed the poorest performance, consistently registering an interruption duration

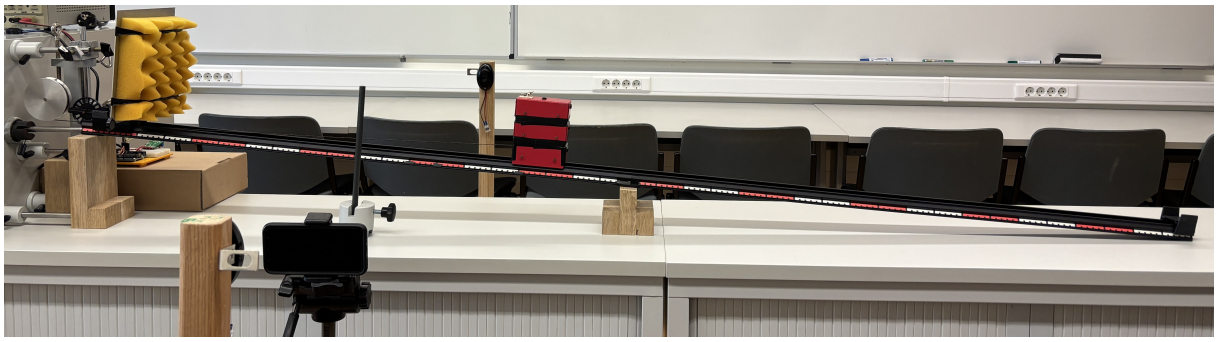

FIGURE 4.1. Experimental setup to test detectors' precision

of 1.5 seconds, even when the interruption was significantly shorter. Detector 2 exhibited a marked decline in accuracy as speed increased. In contrast, Detectors 3, 4, 5, and 6 produced similar results, with Detector 6 displaying the highest relative error.

4.3. Detector Arrangement and Interference Assessment

The system requires two infrared detectors arranged in parallel to determine the direction of pedestrian movement and improve counting accuracy. Two possible configurations are considered:

- *Opposed configuration* – Each detector's transmitter and receiver are placed on opposite sides of the passageway (Figure 4.3a).
- *Crossed Configuration* – Each side of the passage is equipped with a transmitter and receiver from different detectors (Figure 4.3b).

Both configurations are susceptible to interference, though the sources differ. In the opposed configuration, interference may occur due to the wide reception angle of the detectors, which can lead a receiver to unintentionally capture signals from the adjacent transmitter (Figure 4.3a). In the crossed configuration, interference may arise from signal reflections off the body of a pedestrian, causing the receiver to detect unintended signals from the other transmitter (Figure 4.3b).

The minimum allowable distance between detector pairs was experimentally determined to evaluate and compare interference between configurations. A smaller distance between detectors offers multiple advantages, including improved detection accuracy, better individual separation in group scenarios, and reduced spatial requirements for installation, which is critical in constrained environments.

The procedure to determine the minimum separation distance began by placing the detector pair close enough to induce interference. The distance was then gradually increased in small increments until no further interference was detected. The resulting minimum distances required for reliable operation in both configurations are presented in Table 4.4.

Results indicate that Detector 1 performs favorably due to its ability to operate at four distinct frequencies, which facilitates fine-tuning and reduces interference. In contrast, Detectors 2 and 3 were unsuitable for the opposed configuration due to the excessive

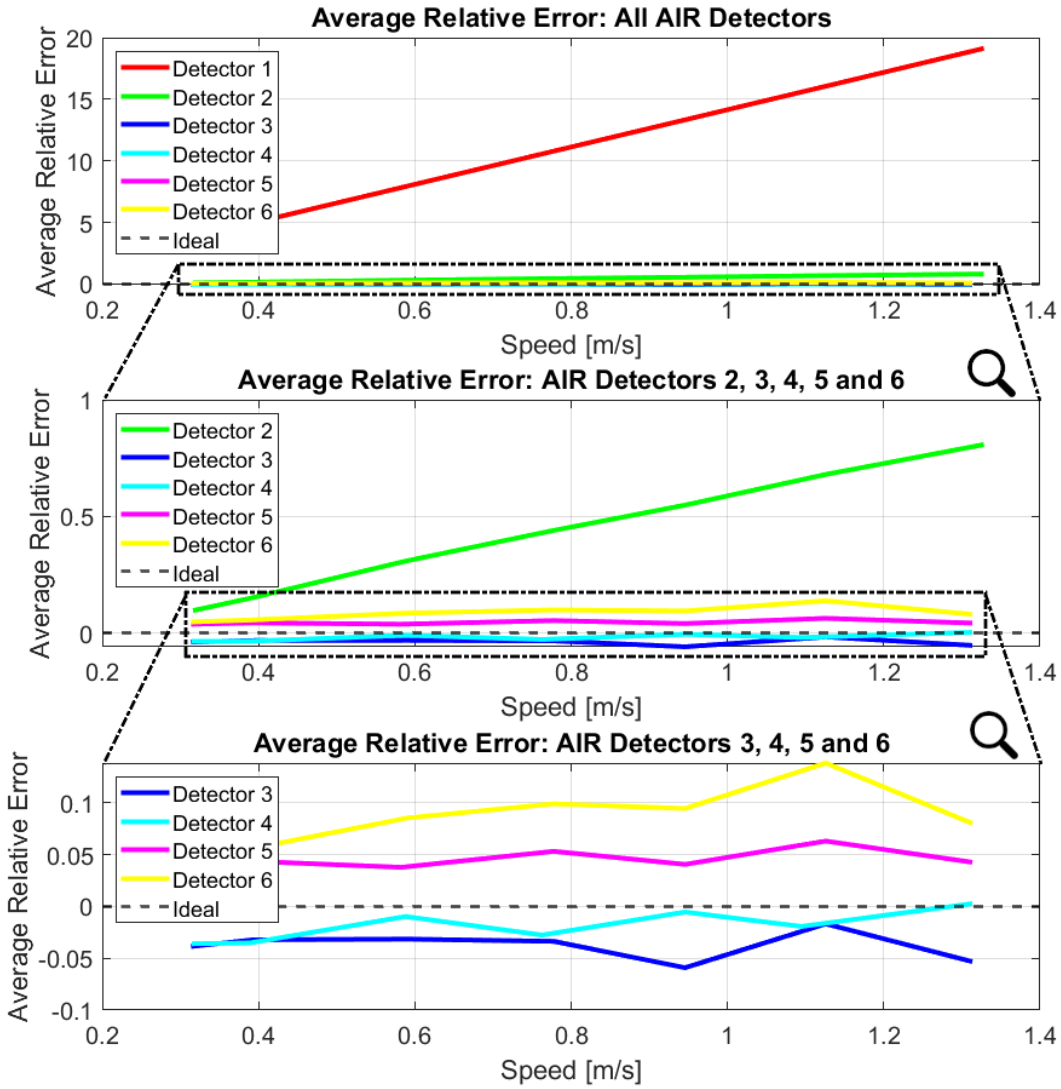

FIGURE 4.2. Detectors' average relative error over speed

TABLE 4.4. Minimum required distance between detectors

Detector ID	Opposed Configuration [cm]	Crossed Configuration [cm]
1	0	0
2	77	32
3	62	12
4	18	18
5	19	5
6	3.5	2

spacing required to eliminate interference. Detector 6, characterized by its high precision, consistently demonstrated optimal performance in both configurations, making it the most effective option for interference mitigation.

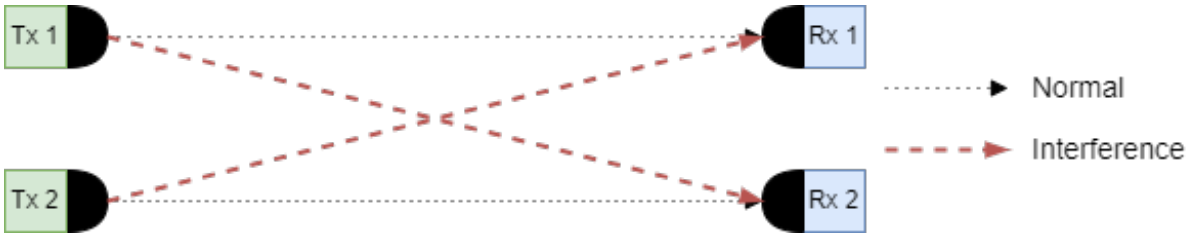

(A) Opposed configuration problem

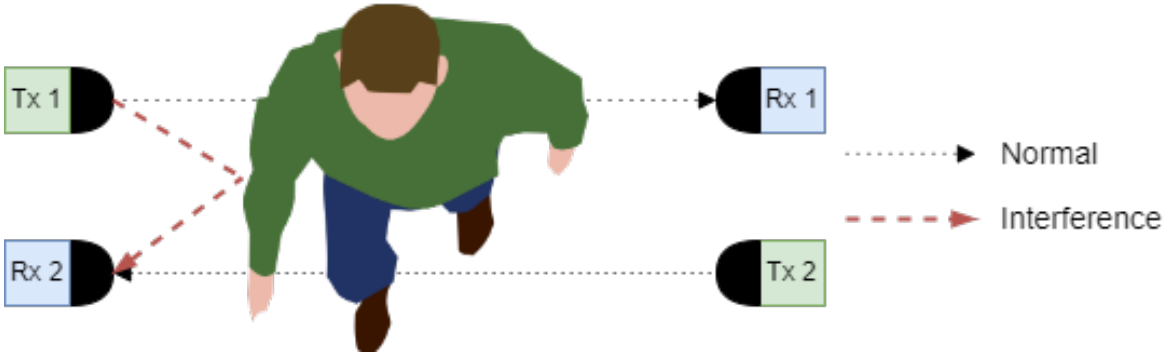

(B) Crossed configuration problem

FIGURE 4.3. Top view – Opposed and crossed configurations

In practice, detectors requiring a minimum spacing of less than 20 centimeters are considered suitable for both the opposed and crossed configurations, as they offer a practical balance between reliable performance and ease of installation.

4.4. Detector Beam Angle Analysis

The horizontal beam angle of infrared detectors is a critical factor influencing accuracy, particularly in environments subject to physical disturbances. Detectors with narrow beam angles are more sensitive to slight misalignments, which may result from unintentional physical disturbances, such as bumps, handling during maintenance, or vibrations from nearby activity. Such deviations can potentially lead to signal loss and potential system malfunction. Conversely, detectors with wider horizontal beam angles exhibit reduced directionality, which may compromise detection accuracy. A broader beam increases the likelihood of registering motion from unintended directions, raising the risk of false positives and erroneous detection.

To assess this characteristic, the maximum horizontal beam angle was measured by independently rotating the transmitter and receiver until the receiver no longer detected the transmitted signal. The angular deviations in each direction were then summed to determine the total beam angle, with results presented in Table 4.5.

The measurements indicate that Detectors 1 and 2 possess the widest horizontal beam angles, making them more susceptible to directionality-related interference. Detector 6, while more directional, exhibited the lowest transmitter angle among all candidates. While this can enhance precision, it also increases vulnerability to slight displacements that may

TABLE 4.5. Horizontal beam angle of detectors

Detector ID	Horizontal beam angle [º]	
	Transmitter (Tx)	Receiver (Rx)
1	185	172
2	207	205
3	25	42
4	48	8
5	17	22
6	2	89

misalign the beam. The remaining detectors displayed moderate beam angles, representing a more favorable balance between directional accuracy and operational stability.

4.5. Comparative Summary

The four key metrics - power consumption, detection accuracy, interference mitigation, and beam angle - underline significant trade-offs in detector selection. A qualitative assessment in Table 4.6 highlights that Detectors 3, 4, 5, and 6 generally outperform detectors 1 and 2.

TABLE 4.6. Qualitative assessment of AIR detectors

Detector ID	Metrics				
	Power Consumption	Accurancy	Interference		Beam angle
			Opposed	Crossed	
1	- -	- -	+ +	+ +	- -
2	- -	-	- -	- -	- -
3	+	+ +	- -	+ -	+ +
4	+	+ +	- -	-	+ +
5	+ -	+ +	+ -	+	+ +
6	+ +	+	+	+	-

In summary, Detector 3 in the Crossed Configuration consistently emerges as the most balanced candidate, combining low-power consumption, reasonable detection accuracy, minimal interference under close spacing, and a well-defined directional beam. Although Detectors 3 and 5 achieved comparable qualitative scores, Detector 3 was ultimately selected for deployment due to its lower power consumption, which directly contributes to improving the sensor's energy autonomy. Detectors 4 and 6 also offer viable alternatives depending on specific design and deployment constraints. In contrast, Detectors 1 and 2 exhibit limitations across multiple metrics, reducing their suitability for compact, low-power, direction-sensitive pedestrian detection systems.

[This page has been intentionally left blank]

CHAPTER 5

System Validation and Performance Evaluation

This chapter validates the proposed pedestrian counting system by evaluating its counting accuracy, the performance of the projected length-based calibration method, and its efficiency in minimizing measurement errors and energy consumption.

This chapter is organized as follows: section 5.1 details the validation of counting accuracy across different test locations, while section 5.2 validates the proposed method for estimating the projected length of objects using the temporal sequence of beam interruptions. Then, section 5.3 describes the calibration and adjustment procedures applied to improve counting precision in real-world scenarios, and section 5.4 focuses on sensor power consumption and autonomy estimation.

5.1. Sensor Count Accuracy Validation

A series of tests were conducted to evaluate the baseline accuracy of the sensor under real operating conditions, with the projected length parameter intentionally excluded to isolate raw counting performance. In doing so, this section addresses Research Question RQ2, which investigates the counting accuracy of the proposed hybrid PIR–AIR sensor across different environmental and spatial configurations.

These tests were carried out in a number of locations, each of which presented distinct spatial and environmental conditions. The primary difference between these sites was the separation distance between the pairs of infrared sensors, which posed a more challenging scenario for detection accuracy. The introduction of wider separations may result in increased problems, as it allows multiple pedestrians to pass simultaneously or side by side.

As outlined in Table 5.1, and demonstrated in Figure 5.1, the chosen locations for the validation experiments are presented to offer a detailed overview of the various configurations and environmental conditions in which the sensor was evaluated during the testing process.

TABLE 5.1. Sensor test locations

ID	Location	Distance [cm]
Narrow (N)	Old Cafeteria, Building 1	70
Medium (M)	Level 3 - Level 4, Building 2	125
Wide (W)	Indoor Crossing between Building 1 and 2	190

Table 5.2 presents the results of the sensor validation experiments conducted across the three test locations. For each site, the table compares the real pedestrian counts

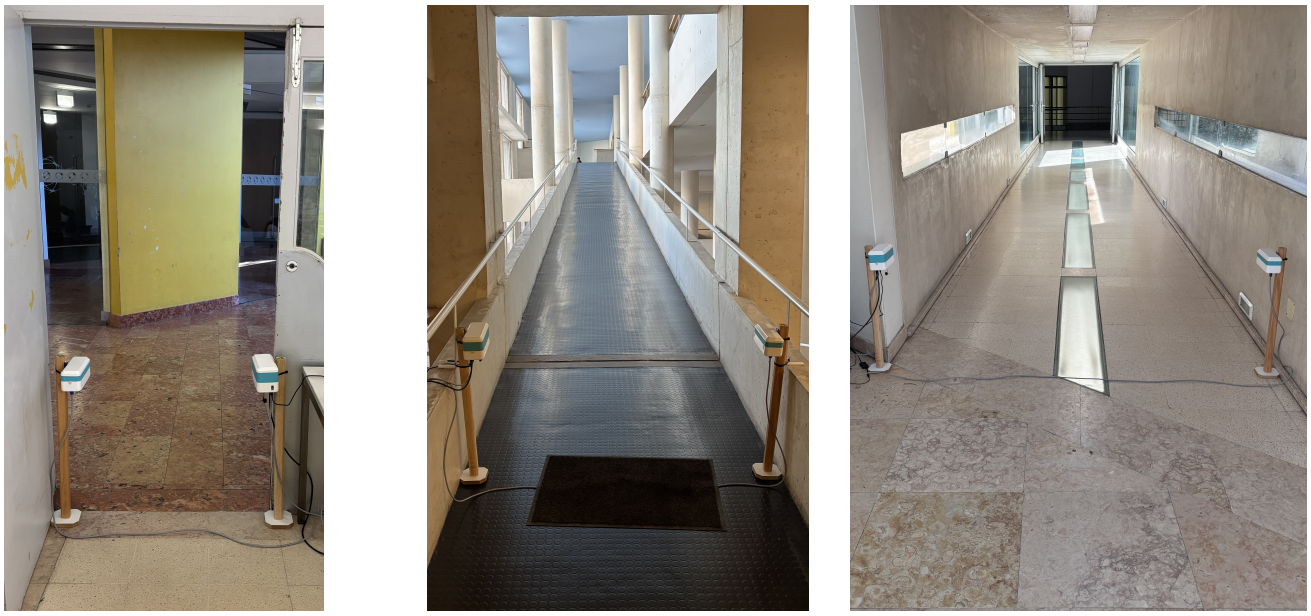

(A) Location N (B) Location M (C) Location W

FIGURE 5.1. Data validation locations

obtained through manual observation with the counts registered by the sensor in both directions of movement. The corresponding percentage error is also provided, offering a quantitative measure of the sensor counting accuracy under these spatial configurations.

TABLE 5.2. Sensor validation results across test locations

Location	Real Counts			Sensor Counts			Error		
	Dir. A	Dir. B	Total	Dir. A	Dir. B	Total	Dir. A	Dir. B	Total
N	50	53	103	57	53	110	14%	0%	7%
M	57	46	103	55	41	96	-4%	-11%	-7%
W	58	46	104	50	33	83	-14%	-28%	-20%

The results demonstrate the variability in the sensor's counting accuracy across different deployment configurations. At Location N, where the distance between the infrared beams was shorter, occasional counting discrepancies occurred. Direct observation during the experiments revealed that objects carried by pedestrians, such as backpacks, water bottles, or jackets, occasionally obstructed the beams and caused false detections. A review of the data revealed that the aforementioned false detections resulted in a projected length of less than 12 centimeters.

In contrast, at Locations M and W, the wider spacing between sensors allowed multiple pedestrians to pass side by side. This often led the system to register a single crossing instead of multiple ones. As the sensor separation increased, the effect became more pronounced, which resulted in the higher error that was observed at Location W. The findings emphasize the influence of beam spacing on detection reliability and underscore the importance of optimizing sensor placement to balance coverage width and counting precision.

5.2. Projected Length Validation

To evaluate the reliability and precision of the proposed technique for estimating the projected length of pedestrians (Figure 3.2), a controlled validation experiment was conducted. The objective was to assess the capability of the temporal-based approach to accurately reproduce the physical dimensions of objects passing through the sensor's detection zone, thus addressing Research Question RQ3, which explores the reliability of projected length estimation from the temporal sequence of beam interruptions.

In order to test the effectiveness of the sensor in measuring human movement, three reference objects with known lengths (25 cm, 34.5 cm, and 60.5 cm) were individually passed through the sensor's beam pair at varying speeds, simulating different walking conditions. To ensure statistical robustness and evaluate the consistency of the measurement process, each object was subjected to 30 independent trials.

The experimental results obtained from these tests provide an empirical basis for validating the proposed estimation method and quantifying its precision under controlled conditions.

The results obtained from the validation tests are presented in Figure 5.2, which illustrates the relationship between the estimated projected length (L) and the average speed (v_{avg}) for all trials.

Each color corresponds to one of the three object sizes that were tested, thereby enabling a visual comparison between the measured projected lengths and the true reference values. A linear model was fitted to the data for each test, with slopes nearing zero, as indicated in Table 5.3.

TABLE 5.3. Linear model fit parameters

	Slope $[s]$	**Intercept** $[cm]$
Test 1	-0.814	55.6
Test 2	0.437	30.6
Test 3	-0.477	23.2

This finding suggests that the estimated projected length remains relatively constant across different crossing speeds, thereby confirming that the method's accuracy is not significantly affected by variations in the object's speed.

While the linear model confirmed that the estimated projected length remains stable across different traversal speeds, it is also important to quantify the deviation of the estimated values from the ground truth. To this objective, a statistical analysis of the normalized error was performed for each test, enabling a more detailed assessment of the method's precision and consistency.

Figures 5.3 (Test 1), 5.4 (Test 2) and 5.5 (Test 3), present the distribution of the normalized error (% of ground truth (GT)) for each of the three tests, together with the corresponding box plots.

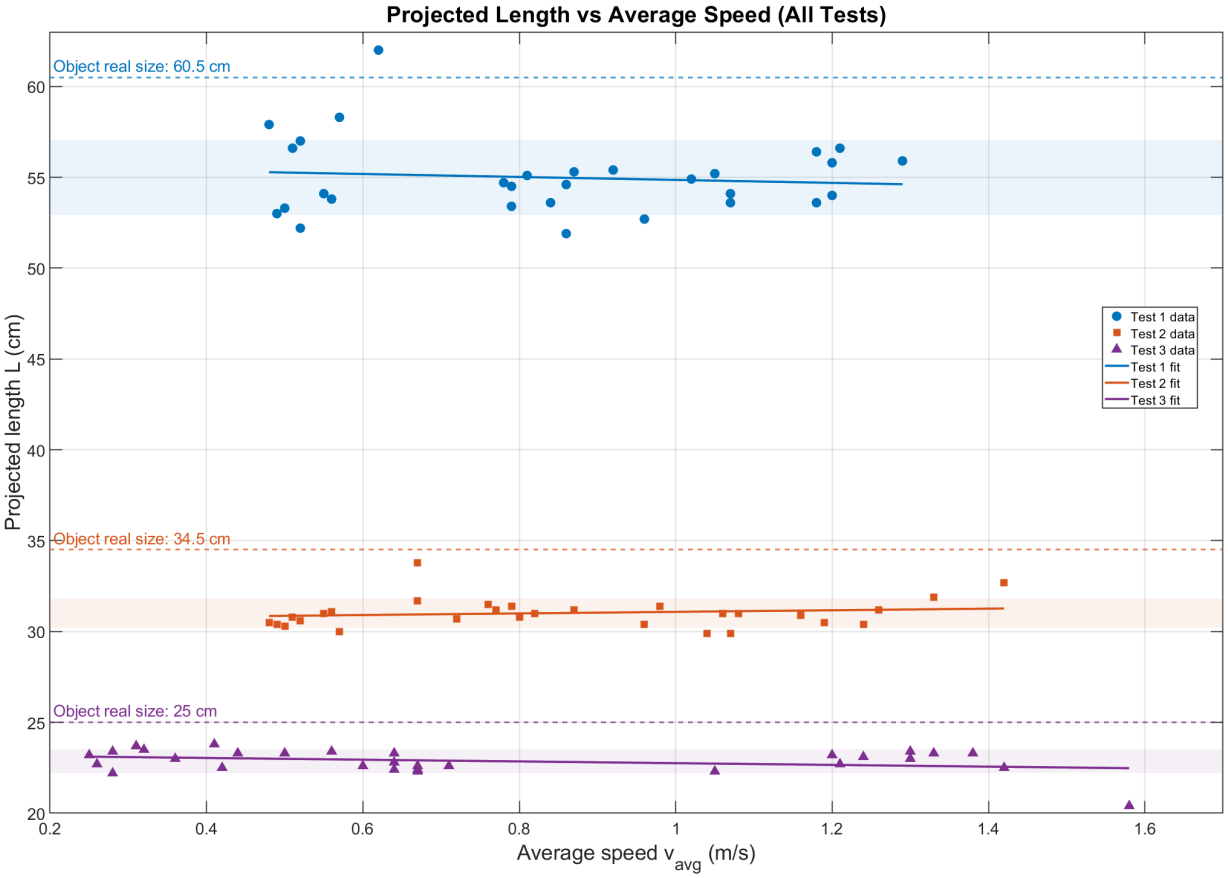

FIGURE 5.2. Projected length as a function of average speed

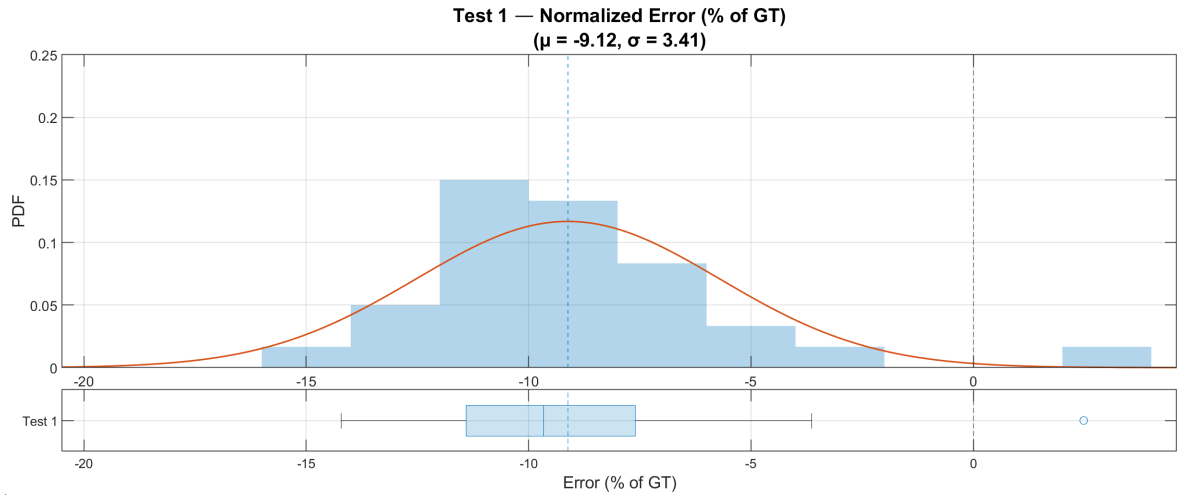

FIGURE 5.3. Test 1 normalized error

The histograms demonstrate that the estimation errors follow an approximately normal distribution, centered around a small negative mean value. This indicates a slight underestimation of the projected length relative to the ground truth. The dispersion of the results, as indicated by the standard deviation, remains within a narrow range across

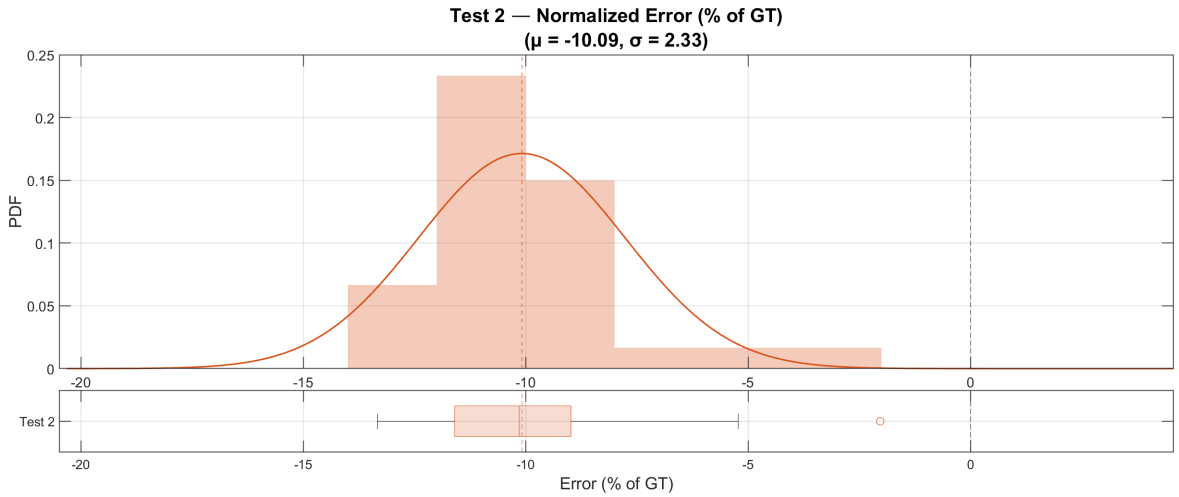

FIGURE 5.4. Test 2 normalized error

FIGURE 5.5. Test 3 normalized error

all tests, thereby confirming the method's consistency. The box plots further emphasize that the majority of estimations fall within a limited error interval, with only a small number of outliers observed.

In Table 5.4, the statistical summary of the normalized error obtained from the projected length validation tests is presented. The table includes the mean, standard deviation, quartiles (Q1 and Q3), interquartile range (IRQ), and median of the error distribution for each test. These metrics provide a quantitative assessment of the estimation consistency and variability, allowing comparison of the system's performance across different object sizes.

The findings demonstrate the efficacy of the proposed approach for estimating object length, providing consistent and reliable measurements across different object sizes. This, in turn, enhances pedestrian counting accuracy and improves the system's ability to distinguish between single and grouped crossings.

TABLE 5.4. Summary statistics of the normalized error (% of ground truth)

	Normalized Error (% of GT)					
	Mean	**Std Dev**	**Q1**	**Q3**	**IRQ**	**Median**
Test 1	-9.12	3.41	-11.4	-7.6	3.8	-9.67
Test 2	-10.09	2.33	-11.59	-8.99	2.6	-10.14
Test 3	-8.51	2.6	-10	-6.8	3.2	-8

5.3. Counting Accuracy Enhancement

To improve the accuracy of the counting mechanism, the projected length method validated in Section 5.1 was employed in additional data collection sessions conducted at the same validation locations, forming the basis for the calibration procedure. In doing so, this section addresses Research Question RQ4, evaluating the effectiveness of the projected length–based calibration approach in minimizing counting errors and improving detection precision.

Figures 5.6 (Location N), 5.7 (Location M) and 5.8 (Location W), present the probability density distributions of the projected length for each test location.

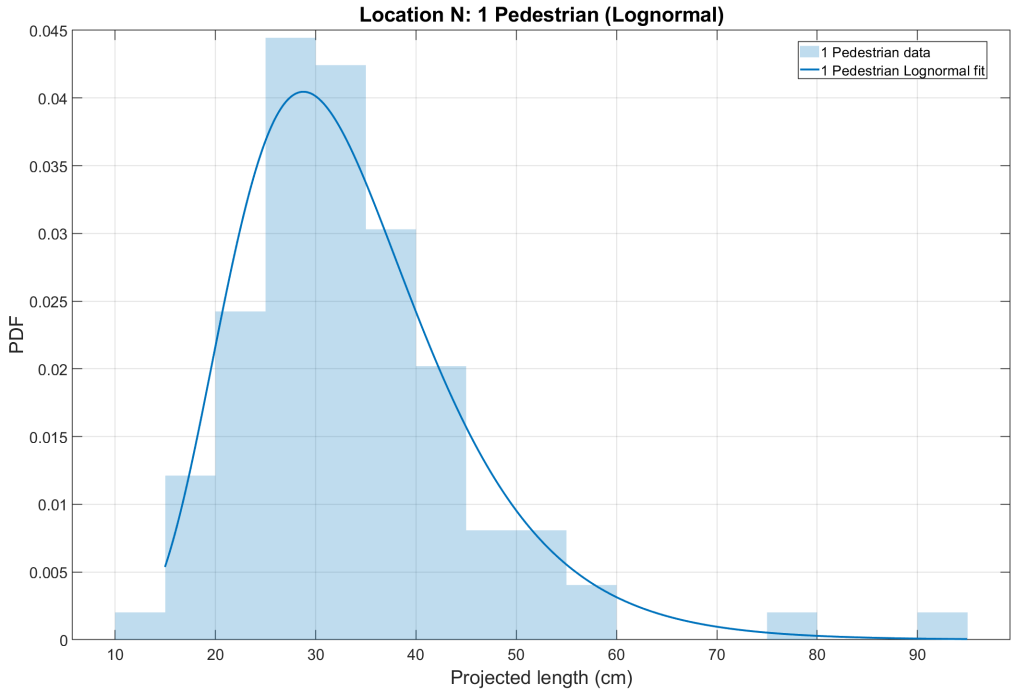

FIGURE 5.6. Location N histogram

For Locations M (125 cm) and W (190 cm), where the distance between the infrared detectors permitted one or two pedestrians to pass concurrently, statistical models were fitted to the distributions of projected length corresponding to both scenarios (1 and 2 pedestrians). The model fit evaluation is presented in A.

The intersection point between the fitted models was subsequently defined as the calibration threshold (L). Projected length values greater than this threshold were interpreted

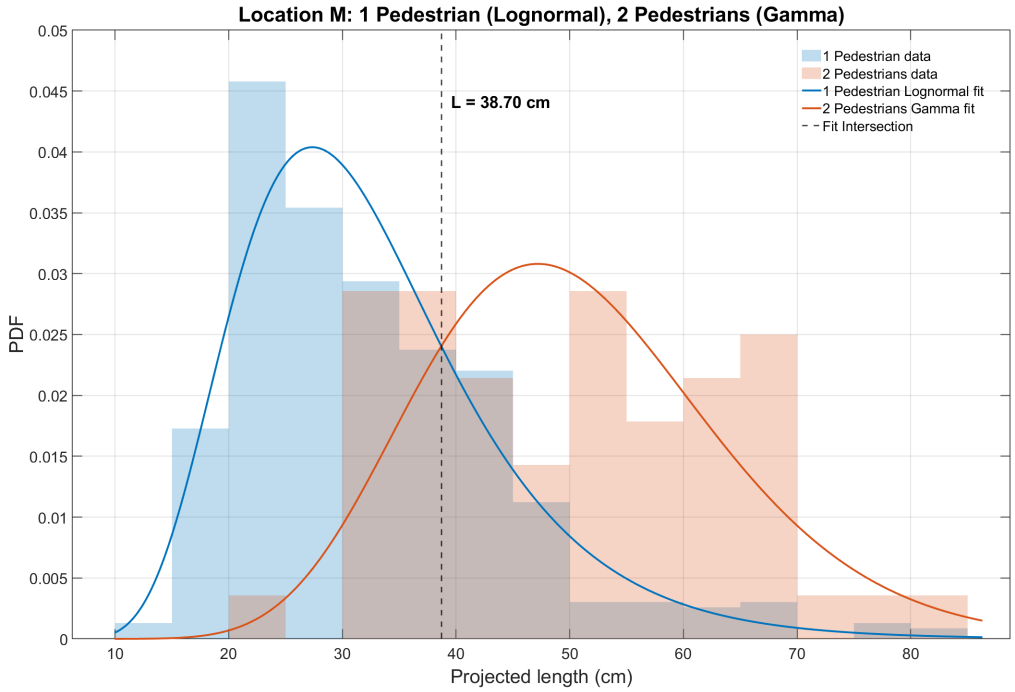

FIGURE 5.7. Location M histogram

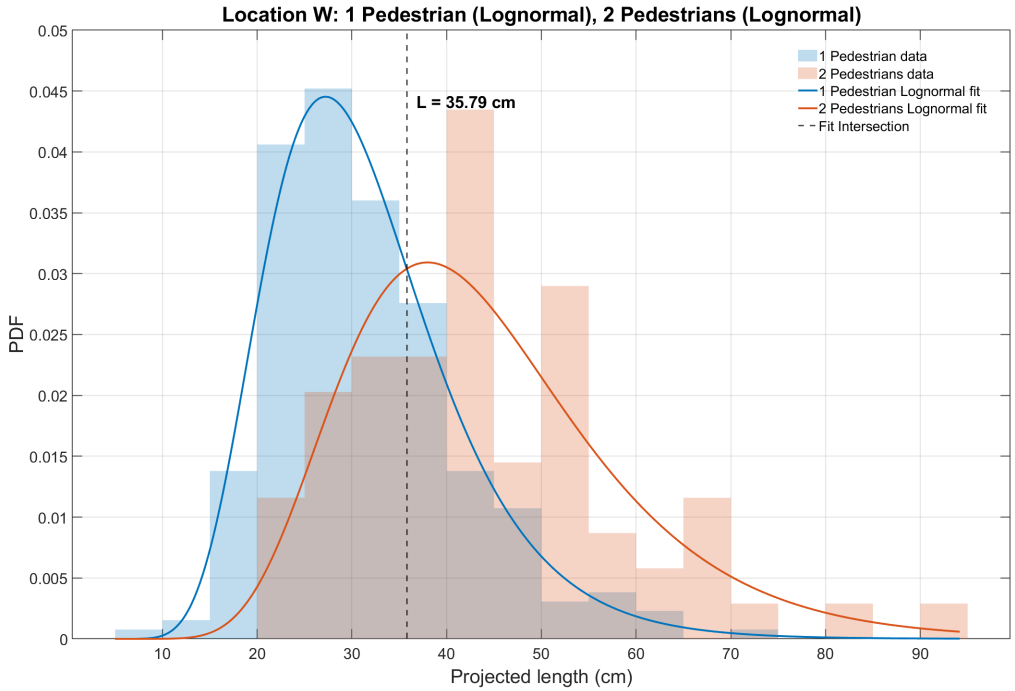

FIGURE 5.8. Location W histogram

as instances of two pedestrians crossing the sensor simultaneously, while smaller values were associated with single crossings.

The obtained thresholds were L=38.7 cm for Location M and L=35.79 cm for Location W. For Location N, where the reduced spacing between sensors prevented simultaneous crossings, only single-pedestrian data were considered.

Furthermore, as evidenced in section 5.1, false detections caused by minor obstructions such as hands or bags were detected as lengths below 12 centimeters. Consequently, values falling below this threshold were excluded from the analysis.

After applying these adjustments, the previously collected validation data were calibrated, and the resulting performance improvements are summarized in Table 5.5.

TABLE 5.5. Sensor validation error after calibration

Location	Real Counts			Sensor Counts			Error		
	Dir. A	Dir. B	Total	Dir. A	Dir. B	Total	Dir. A	Dir. B	Total
N	50	53	103	48	52	100	-4%	-2%	-3%
M	57	46	103	55	43	98	5%	4%	5%
W	58	46	104	50	42	92	9%	7%	8%

Table 5.6 presents a comparison of the counting errors obtained before and after applying the calibration procedure.

TABLE 5.6. Error before and after calibration

Location	Previous Error			Calibrated Error		
	Dir. A	Dir. B	Total	Dir. A	Dir. B	Total
N	14%	0%	7%	-4%	-2%	-3%
M	-4%	-11%	-7%	5%	4%	5%
W	-14%	-28%	-20%	9%	7%	8%

The implementation of the calibration strategy resulted in a substantial enhancement in counting accuracy across all test locations, with the majority of error values approaching the ideal value of 0%. At Location N, the total error exhibited a decrease from 7% to -3%, with Dir. A demonstrating an improvement from 14% to -4%. However, a slight deterioration was observed in Dir. B, where the error increased marginally from 0% to -2%. At Location M, the total error demonstrated an improvement, shifting from -7% to 5%. Additionally, a notable shift was observed in the Dir. A and Dir. B errors, which transitioned from -4% and -11% to 5% and 4%, respectively. Finally, Location W, which initially exhibited the most significant deviations (20% Total, 14% in Dir. A, and 28% in Dir. B), demonstrated the most substantial enhancement following calibration, reaching 8%, 9%, and 7%, respectively.

The results indicate a clear convergence toward zero error, thereby confirming the efficacy of the proposed calibration method in effectively mitigating systematic deviations in the counting process.

5.4. Sensor Consumption

Power consumption constitutes a key performance metric of the proposed system, especially considering its intended deployment in environments with limited power availability and restricted maintenance access. This section analyzes the energy requirements of the sensor during both active and sleep phases to evaluate its efficiency and estimate its expected operational autonomy. In doing so, it addresses Research Question RQ5, which investigates the energy performance of the proposed system relative to conventional AIR-only pedestrian counting solutions.

Table 5.7 presents the average power consumption of the complete sensor assembly, which includes the microcontroller, PIR and AIR detectors, DC converter, and optocoupler.

TABLE 5.7. Average sensor power consumption

Phase	**Power Consumption [mW]**
Sleep	166.04
Active	918.06

The active phase value is derived from an average of multiple readings, as the current draw fluctuates during data processing and wireless communication. This provides a representative estimate of the system's overall power demand during operation, in contrast to the stable consumption observed in the sleep phase.

Using the values presented in Table 5.7, the autonomy of the sensor can be predicted using Equations 5.1 and 5.2.

$$P_{avg} = P_{sleep} \cdot (1 - d) + P_{active} \cdot d \tag{5.1}$$

P_{avg}: Average Power Consumption $[mW]$
P_{sleep}: Sleep Power Consumption $[mW]$
P_{active}: Active Power Consumption $[mW]$
d: Duty cycle

$$Autonomy(days) \approx \frac{E \cdot \eta}{P_{avg} \cdot 24h} \tag{5.2}$$

E: Nominal Battery Energy
η: Efficiency

Assuming a 96 Wh battery and an overall system efficiency of 75% as reported in [27], the expected operational autonomy of the sensor under different duty cycles (proportion of time the sensor remains active) is shown in Figure 5.9.

The analysis predicts that the duty cycle is a significant factor in enhancing the energy performance of the system. It has been predicted that, by maintaining a low average power

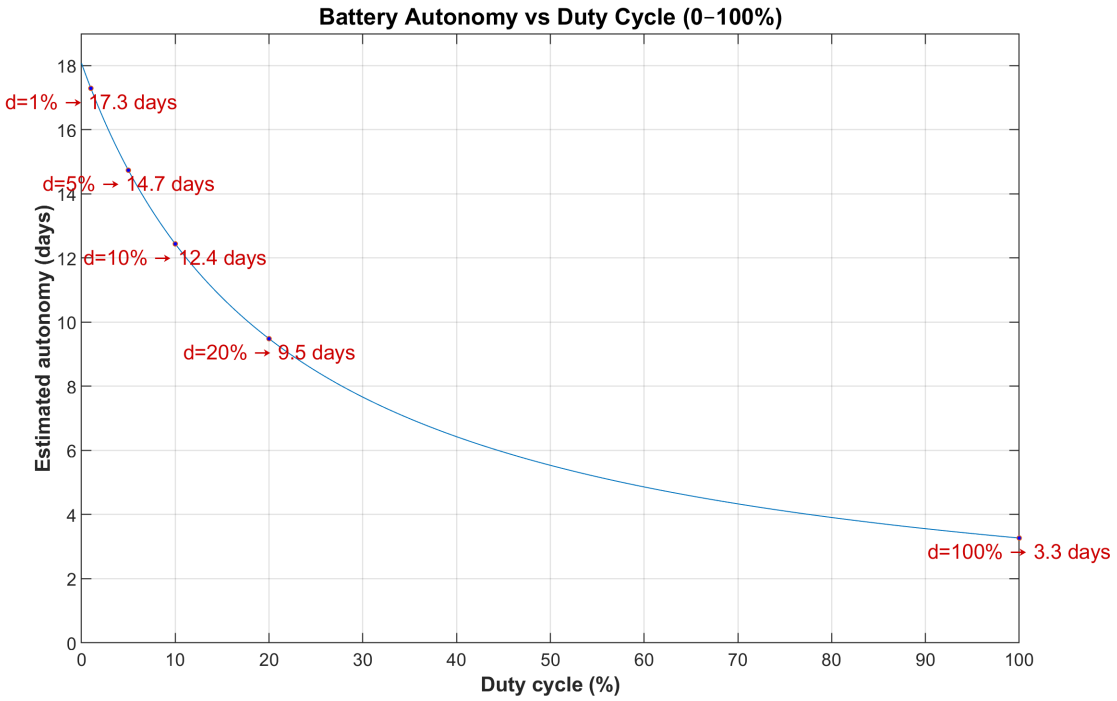

FIGURE 5.9. Sensor autonomy

draw, the sensor is capable of achieving up to 18 days of continuous operation from a single 96 Wh battery in low traffic situations.

This extended autonomy serves to reinforce the practicality of the system for real-world deployments in smart-city and remote-area scenarios, where maintenance frequency and power availability are critical constraints.

CHAPTER 6

Conclusion and Future Work

This chapter concludes the dissertation and proposes directions for future work focused on the continued development and dissemination of the research.

6.1. Conclusion

This dissertation presented the development of a low-cost, energy-efficient pedestrian monitoring system supported by sensors that employ two AIR detectors arranged in parallel, triggered by PIR detectors, to optimize power usage. By selectively activating the AIR modules and associated processing and communication only when motion is detected, the system sensors achieve a fivefold increase in operational autonomy compared with conventional AIR-only solutions. Furthermore, flexible uplink communication options, including Wi-Fi and LoRaWAN, facilitate broad adaptability to diverse deployment scenarios.

The proposed system uses open-source technologies and low-cost hardware to detect pedestrian movement and determine their direction. It enhances crowd management and safety by enabling real-time monitoring of pedestrian flow, triggering alarms, and providing longitudinal data that can be analyzed in a graphical dashboard.

A comprehensive comparison of AIRs revealed that specific models demonstrate superior power efficiency, accuracy, and resistance to mutual interference. The most suitable AIR was selected based on experimental validation, ensuring optimal performance in real-world deployment.

The system's capacity to accurately count pedestrians, determine their direction and speed, and operate in environments with limited infrastructure was validated through field experiments. The proposed methodology for length estimation demonstrated enhanced accuracy through the differentiation between single and simultaneous crossings, thereby minimizing total counting error. These results confirm that the proposed system is a robust, autonomous, and privacy-preserving solution for monitoring pedestrians in urban and remote contexts.

Through this research, all research questions (RQ1–RQ5) were successfully addressed. Specifically, RQ1 identified the most suitable AIR detector balancing performance and energy efficiency; RQ2 validated the counting accuracy of the hybrid PIR–AIR system in real environments; RQ3 confirmed the reliability of the temporal-based projected length estimation method; RQ4 demonstrated the effectiveness of the calibration procedure in enhancing counting precision; and RQ5 established the system's energy efficiency and superior autonomy relative to conventional AIR-only solutions.

Overall, this research contributes to the advancement of low-power intelligent sensing for mobility analysis and environmental monitoring by addressing the gap between academic prototypes and practical IoT deployments.

6.2. Future Work

The system achieved promising results in controlled experiments. Several enhancements can be pursued to further improve its performance for large-scale deployment.

First, the hardware components can be optimized to extend battery autonomy beyond the current configuration. Subsequent iterations of the system should investigate the use of microcontrollers and PIR detectors that exhibit reduced power consumption, while ensuring that sufficient processing capability and detection range are maintained. The evaluation of alternative solutions has the potential to further reduce the average power draw and extend the operational lifespan of the sensor in off-grid environments.

Secondly, further investigation should assess whether the projected length (L) calibration threshold varies with the distance between sensor pairs. This analysis would help determine if the threshold is dependent on the geometric configuration of the detectors, thereby refining the system's calibration process and improving its adaptability to different installation scenarios.

Thirdly, the system could be enhanced with an auto-learning calibration mechanism for the projected length threshold. This capability would allow the sensor to dynamically adjust the threshold used to classify multi-person crossings, continuously updating it based on observed data patterns over time. Such an adaptive mechanism would improve counting accuracy across different environmental conditions and pedestrian behaviors, while eliminating the need for manual recalibration.

Finally, real-world deployment in locations such as the Tagus Estuary Bird Observation and Conservation Area (EVOA) is a crucial next step to validate the sensor's robustness under environmental variability. Conducting field trials in a natural environment would facilitate long-term performance evaluation, ensure reliable communication under limited connectivity, and validate the system's feasibility for sustainable visitor monitoring in ecologically sensitive areas.

6.3. Communication

The dissemination of this research was carried out through several actions targeting both the professional and scientific communities. Within the professional community, the results will be shared through the publication of a technical report under the MoniCrowd project, as well as the release of the developed source code in an open-access GitHub repository, enabling transparency, reproducibility, and further technological development.

In the scientific community, the research was presented and discussed at the STARS Symposium and at the International Conference on Ubiquitous and Future Networks (ICUFN) [8]. Additionally, the corresponding article was published in the IEEE Xplore

Digital Library, accessible online under DOI: 10.1109/ICUFN65838.2025.11170080, ensuring global visibility and long-term accessibility of the research outcomes.

[This page has been intentionally left blank]

References

[1] Y.-F. Leung, A. Spenceley, G. Hvenegaard, R. Buckley, and C. Groves, *Tourism and visitor management in protected areas: Guidelines for sustainability*. Intern. Union for Conservation of Nature, 2018, vol. 27.

[2] F. Brito e Abreu et al., "A digital transformation approach to scaffold tourism crowding management: pre-factum, on-factum, and post-factum", in *ECTI DAMT & NCON*, IEEE, Chiangmai, Thailand, Jan. 2024, pp. 586–591, ISBN: 979-8-3503-1824-1. DOI: 10.1109/ECTIDAMTNCON60518.2024.10480056

[3] F. B. e Abreu, R. N. Marinheiro, J. Oliveira, and T. M. Santos, "Quality-driven edge-to-cloud architecture for crowd monitoring with wi-fi sensing", in *Proceedings of the IEEE Annual Congress on Artificial Intelligence of Things (IEEE AIoT)*, Osaka, Japan: IEEE, Dec. 2025, pp. 1–7.

[4] R. N. Marinheiro, F. B. e Abreu, T. Vieira, and M. Martins, "Adaptive crowd sensing with privacy-preserving wifi fingerprinting", in *Proceedings of the 9th IEEE International Conference on Smart Internet of Things (SmartIoT 2025)*, Sydney, Australia: IEEE, Nov. 2025, pp. 1–8.

[5] C.-Y. Chan and F. Bu, "Literature Review of Pedestrian Detection Technologies and Sensor Survey", Institute of Transportation Studies, Univ. of California, Berkeley, Technical Report UCB-ITS-PRR-2005-22, 2005.

[6] S. T. Kouyoumdjieva, P. Danielis, and G. Karlsson, "Survey of Non-Image-Based Approaches for Counting People", *IEEE Communications Surveys and Tutorials*, vol. 22, pp. 1305–1336, 2 Apr. 2020, ISSN: 1553877X. DOI: 10.1109/COMST.2019.2902824

[7] K. Peffers, T. Tuunanen, M. A. Rothenberger, and S. Chatterjee, "A Design Science Research Methodology for Information Systems Research", *Journal of Management Information Systems*, vol. 24, no. 3, pp. 45–77, 2007. DOI: 10.2753/MIS0742-1222240302

[8] T. Vieira, S. Paiva, R. N. Marinheiro, and F. B. e Abreu, "Building Optimized Wireless Pedestrian Counting Sensors Combining Passive and Active Technologies", in *Proceedings of the Sixteenth International Conference on Ubiquitous and Future Networks (ICUFN)*, IEEE, Jul. 2025, pp. 574–581, ISBN: 979-8-3315-2487-6. DOI: 10.1109/ICUFN65838.2025.11170080

[9] N. Buch, S. A. Velastin, and J. Orwell, "A Review of Computer Vision Techniques for the Analysis of Urban Traffic", *IEEE Transactions on Intelligent Transportation*

Systems, vol. 12, pp. 920–939, 3 Sep. 2011, ISSN: 1524-9050. DOI: 10.1109/TITS.2011.2119372

[10] M. S. A. Muthanna, Y. T. Lyachek, A. M. O. Musaeed, Y. A. H. Esmail, and A. B. M. Adam, "Smart System of a Real-Time Pedestrian Detection for Smart City", in *Proceedings of the Conference of Russian Young Researchers in Electrical and Electronic Engineering (EIConRus)*, IEEE, Jan. 2020, pp. 45–50, ISBN: 978-1-7281-5761-0. DOI: 10.1109/EIConRus49466.2020.9039333

[11] F. Akhter, S. Khadivizand, J. Lodyga, H. R. Siddiquei, M. E. E. Alahi, and S. Mukhopadhyay, "Design and Development of an IoT enabled Pedestrian Counting and Environmental Monitoring System for a Smart City", in *Proceedings of the 13th International Conference on Sensing Technology (ICST)*, IEEE, Dec. 2019, pp. 1–6, ISBN: 978-1-7281-4807-6. DOI: 10.1109/ICST46873.2019.9047695

[12] Z. Li, Z. Jia, J. Yang, and N. Kasabov, "Low Illumination Video Image Enhancement", *IEEE Photonics Journal*, vol. 12, 4 Aug. 2020, ISSN: 19430655. DOI: 10.1109/JPHOT.2020.3010966

[13] M. Casares, A. Pinto, Y. Wang, and S. Velipasalar, "Power consumption and performance analysis of object tracking and event detection with wireless embedded smart cameras", in *Proceedings of the 3rd International Conference on Signal Processing and Communication Systems*, IEEE, Sep. 2009, pp. 1–8, ISBN: 978-1-4244-4473-1. DOI: 10.1109/ICSPCS.2009.5306375

[14] S. A. Velastin, R. Fernández, J. E. Espinosa, and A. Bay, "Detecting, tracking and counting people getting on/off a metropolitan train using a standard video camera", *Sensors (Switzerland)*, vol. 20, pp. 1–20, 21 Nov. 2020, ISSN: 14248220. DOI: 10.3390/s20216251

[15] L. Spinello and K. O. Arras, "People detection in RGB-D data", in *Proceedings of the IEEE/RSJ International Conference on Intelligent Robots and Systems*, IEEE, Sep. 2011, pp. 3838–3843, ISBN: 978-1-61284-456-5. DOI: 10.1109/IROS.2011.6095074

[16] T. W. Hnat, E. Griffiths, R. Dawson, and K. Whitehouse, "Doorjamb", in *Proceedings of the 10th ACM Conference on Embedded Network Sensor Systems*, ACM, Nov. 2012, pp. 309–322, ISBN: 9781450311694. DOI: 10.1145/2426656.2426687

[17] J. W. Choi, X. Quan, and S. H. Cho, "Bi-Directional Passing People Counting System Based on IR-UWB Radar Sensors", *IEEE Internet of Things Journal*, vol. 5, pp. 512–522, 2 Apr. 2018, ISSN: 23274662. DOI: 10.1109/JIOT.2017.2714181

[18] K. C. Sahoo and U. C. Pati, "IoT based intrusion detection system using PIR sensor", in *Proceedings of the 2nd IEEE International Conference on Recent Trends in Electronics, Information & Communication Technology (RTEICT)*, IEEE, May 2017, pp. 1641–1645, ISBN: 978-1-5090-3704-9. DOI: 10.1109/RTEICT.2017.8256877

[19] J. Andrews, M. Kowsika, A. Vakil, and J. Li, "A Motion Induced Passive Infrared (PIR) Sensor for Stationary Human Occupancy Detection", in *Proceedings of the IEEE/ION Position, Location and Navigation Symposium (PLANS)*, IEEE, Apr.

2020, pp. 1295–1304, ISBN: 978-1-7281-0244-3. DOI: 10.1109/PLANS46316.2020.9109909

[20] C. Perra, A. Kumar, M. Losito, P. Pirino, M. Moradpour, and G. Gatto, "Monitoring indoor people presence in buildings using low-cost infrared sensor array in doorways", *Sensors*, vol. 21, 12 2021, ISSN: 14248220. DOI: 10.3390/s21124062

[21] H. Yang, K. Ozbay, and B. Bartin, "Enhancing the quality of infrared-based automatic pedestrian sensor data by nonparametric statistical method", *Transportation Research Record*, pp. 11–17, 2264 Dec. 2011, ISSN: 03611981. DOI: 10.3141/2264-02

[22] Z. Fang, Y. Xinwei, G. Junhua, and Y. Ruixia, "A new method for people-counting based on support vector machine", in *Proceedings of the Asia-Pacific Conference on Information Processing (APCIP)*, vol. 1, 2009, pp. 109–112, ISBN: 9780769536996. DOI: 10.1109/APCIP.2009.36

[23] A. Sirikham, P. Kirdpipat, and Y. Saeear, "Development of Bi-Directional Portable People Counter System based IoT", in *Proceedings of the 9th International Electrical Engineering Congress (iEECON)*, Institute of Electrical and Electronics Engineers Inc., Mar. 2021, pp. 503–506, ISBN: 9781728195841. DOI: 10.1109/iEECON51072.2021.9440295

[24] T. M. dos Santos, R. N. Marinheiro, and F. B. e Abreu, "Wireless Crowd Detection for Smart Overtourism Mitigation", in *Smart Life and Smart Life Engineering*, Springer Nature Switzerland, 2025, pp. 237–258. DOI: 10.1007/978-3-031-75887-4_11

[25] L. Wu and B. Coifman, "Improved vehicle classification from dual-loop detectors in congested traffic", *Transportation Research Part C: Emerging Technologies*, vol. 46, pp. 222–234, Sep. 2014, ISSN: 0968090X. DOI: 10.1016/j.trc.2014.04.015

[26] E. M. Murtagh, J. L. Mair, E. Aguiar, C. Tudor-Locke, and M. H. Murphy, "Outdoor Walking Speeds of Apparently Healthy Adults: A Systematic Review and Meta-analysis", *Sports Medicine*, vol. 51, pp. 125–141, 1 2021, ISSN: 0112-1642. DOI: 10.1007/s40279-020-01351-3

[27] G. J. May, A. Davidson, and B. Monahov, "Lead batteries for utility energy storage: A review", *Journal of Energy Storage*, vol. 15, pp. 145–157, 2 Feb. 2018, ISSN: 2352152X. DOI: 10.1016/j.est.2017.11.008

[28] K. Burnham and D. Anderson, "Multimodel Inference: understanding AIC and BIC in Model Selection", *Sociological Methods Research*, vol. 33, pp. 261–304, Jan. 2004.

[29] F. J. M. Jr., "The Kolmogorov-Smirnov Test for Goodness of Fit", *Journal of the American Statistical Association*, vol. 46, no. 253, pp. 68–78, 1951. DOI: 10.1080/01621459.1951.10500769

[This page has been intentionally left blank]

APPENDIX A

Fit Model Evaluation

The quality of each fitted distribution was evaluated using three measures: the Akaike Information Criterion (AIC), the Bayesian Information Criterion (BIC), and the Kolmogorov Smirnov (KS) test.

The AIC and BIC measure how well a model fits the data while penalizing unnecessary complexity, where k is the number of model parameters [28]. Lower AIC and BIC values indicate better models, with the minimum value identifying the preferred distribution.

The KS test compares the empirical and theoretical cumulative distributions [29]. It provides a distance value D and a p-value. A smaller D means the fitted model closely matches the data, and a larger p (typically greater than 0.05) means the model cannot be rejected as a good fit.

In summary, the best-fit model is the one with the lowest AIC and BIC and a KS test showing small D and high p-value.

Table A.1 summarizes the goodness-of-fit results for Location N (70 cm), listing the tested distributions in order of performance for single-pedestrian crossings.

TABLE A.1. Location N - 1 pedestrian

Distribution	**k**	**AIC**	**BIC**	**KS**	
				D	**p**
Lognormal	2	747.53	752.72	0.054	0.92
Gamma	2	752.84	758.03	0.059	0.86
Weibull	2	776.78	781.97	0.099	0.26
Normal	2	777.22	782.41	0.106	0.2

Tables A.2 and A.3 summarize the goodness-of-fit results for Location M (125 cm), listing the tested distributions in order of performance for single-pedestrian and double-pedestrian crossings, respectively.

TABLE A.2. Location M - 1 pedestrian

Distribution	**k**	**AIC**	**BIC**	**KS**	
				D	**p**
Lognormal	2	3491.5	3499.8	0.059	0.075
Gamma	2	3518.3	3526.6	0.076	0.009
Weibull	2	3604.9	3613..2	0.103	9.56e-5
Normal	2	3621.3	3629.6	0.1	1.67e-4

TABLE A.3. Location M - 2 pedestrians

Distribution	k	AIC	BIC	KS	
				D	p
Gamma	2	450.47	454.52	0.085	0.78
Lognormal	2	451.29	455.34	0.086	0.77
Normal	2	451.77	455.82	0.099	0.61
Weibull	2	452.15	456.2	0.01	0.6

Tables A.4 and A.5 summarize the goodness-of-fit results for Location W (190 cm), listing the tested distributions in order of performance for single-pedestrian and double-pedestrian crossings, respectively.

TABLE A.4. Location W - 1 pedestrian

Distribution	k	AIC	BIC	KS	
				D	p
Lognormal	2	1913.8	1921	0.029	0.98
Gamma	2	1915.6	1922.7	0.048	0.57
Normal	2	1945.7	1952.8	0.081	0.06
Weibull	2	1949.4	1956.6	0.079	0.08

TABLE A.5. Location W - 2 pedestrians

Distribution	k	AIC	BIC	KS	
				D	p
Lognormal	2	558.91	563.38	0.074	0.81
Gamma	2	559.51	563.98	0.085	0.68
Normal	2	567.31	571.77	0.117	0.28
Weibull	2	567.63	572.1	0.126	0.2